NASA TECHNICAL MEMORANDUM

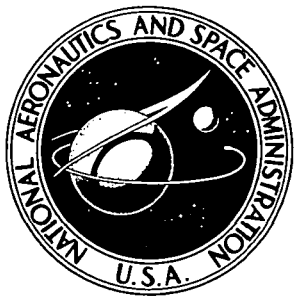

NASA TM X-3413

NASA TM X-3413

ACOUSTIC, PERFORMANCE, AND WAKE SURVEY MEASUREMENTS OF A LOBED VELOCITY-DECAYER NOZZLE INSTALLED ON A QUIETED TF-34 TURBOFAN ENGINE

Nick E. Samanich and Laurence J. Heidelberg

Lewis Research Center
Cleveland, Ohio 44135

NATIONAL AERONAUTICS AND SPACE ADMINISTRATION • WASHINGTON, D. C. • AUGUST 1976

1. Report No. NASA TM X-3413	2. Government Accession No.	3. Recipient's Catalog No.
4. Title and Subtitle ACOUSTIC, PERFORMANCE, AND WAKE SURVEY MEASUREMENTS OF A LOBED VELOCITY-DECAYER NOZZLE INSTALLED ON A QUIETED TF-34 TURBOFAN ENGINE		5. Report Date August 1976 6. Performing Organization Code
7. Author(s) Nick E. Samanich and Laurence J. Heidelberg		8. Performing Organization Report No. E-8676
9. Performing Organization Name and Address Lewis Research Center National Aeronautics and Space Administration Cleveland, Ohio 44135		10. Work Unit No. 505-04 11. Contract or Grant No.
12. Sponsoring Agency Name and Address National Aeronautics and Space Administration Washington, D.C. 20546		13. Type of Report and Period Covered Technical Memorandum 14. Sponsoring Agency Code
15. Supplementary Notes		

16. Abstract

Results for three velocity-decayer nozzle configurations are compared with those obtained with a separate-flow coannular nozzle tested on the same quieted turbofan engine. Peak sideline noise, which occurred 110^{o} from the inlet, was 2 to 4 dB louder than with the coannular nozzle at the same ideal effective exhaust velocity and 8 to 11 dB louder at the same thrust level. The decayer nozzles produced an increase in loss equivalent to about 4 percent of the engine thrust and also increased the effective exhaust velocity of the engine. The exhaust decayed to 0.35 of its peak velocity, compared with no decay for the coannular nozzle, within 3 equivalent nozzle diameters of the exit. The peak exhaust gas temperature was 400 K (720^{o} R) lower for the decayer configuration at the same location. The increase in perceived noise level for the decayer nozzles as compared with the coannular nozzle was attributed to the increase in exhaust velocity and the shift in peak spectrum frequency produced by these nozzles.

17. Key Words (Suggested by Author(s))	18. Distribution Statement
Air breathing engines Noise reduction Acoustics Nozzles	Unclassified - unlimited STAR Category 07

19. Security Classif. (of this report)	20. Security Classif. (of this page)	21. No. of Pages	22. Price*
Unclassified	Unclassified	46	$4.00

* For sale by the National Technical Information Service, Springfield, Virginia 22161

ACOUSTIC, PERFORMANCE, AND WAKE SURVEY MEASUREMENTS OF A LOBED VELOCITY-DECAYER NOZZLE INSTALLED ON A QUIETED TF-34 TURBOFAN ENGINE

by Nick E. Samanich and Laurence J. Heidelberg

Lewis Research Center

SUMMARY

Far-field acoustic, static performance, and wake survey measurements were made of a quieted TF-34 turbofan engine with a 12-lobe velocity-decayer nozzle. A mixed-flow exhaust system was used, with the engine core flow discharged internally. Tests included both an annular and a mixer core nozzle. Decayer exit area was also varied. The results were compared with those obtained with a separate-flow coannular nozzle tested on the same engine.

Along a constant radius from the exit, peak noise occurred 140° from the inlet; however, when extrapolated to a sideline and converted to a perceived noise level, the peak occurred 110° from the inlet. The mixer-decayer nozzle was 2 decibels noisier than the coannular nozzle at comparable effective exhaust velocities and 8 decibels noisier at comparable thrust levels.

The increase in internal losses associated with the decayer nozzle configurations was equivalent to about 4 percent of the engine gross thrust. All configurations had greater effective exhaust velocities than the coannular nozzle at the same power setting. This increase in effective exhaust velocity was the primary cause of the higher noise level of the decayer nozzles.

Wake surveys showed that the exhaust decayed to 0.35 of its peak velocity, as compared with no decay for the coannular nozzle, within 3 equivalent nozzle diameters from the exit. The peak exhaust gas temperature was 400 K (720° R) lower for the decayer configuration at the same location. The degree of velocity decay was insensitive to whether or not an internal mixer was used and to a variation of 12 percent in decayer exit area.

INTRODUCTION

Aircraft operating noise is becoming an ever increasing problem resulting in stringent restrictions being placed on both operation and aircraft design. This problem is particularly severe for short-haul aircraft operating near heavily populated areas. Because of the relatively small airfields in these areas, aircraft designers are considering some form of supplementary powered lift as a future requirement for these aircraft. Unfortunately, associated with powered lift systems are additional noise sources not present in conventional lifting aircraft. Preliminary investigations indicate that these noise sources can be the dominant noise sources and may well dictate the choice of the powered lift system.

One method of achieving lift augmentation is the externally blown flap system (EBF), where the engines are located such that the exhaust gases impinge on (or are directed toward) the wing-flap system and are deflected downward. Lift augmentation comes about by the reaction to the downward jet deflection and also by the inducing of a favorable pressure distribution on the wing-flap system. However, model tests have shown that the interaction of the exhaust and the wing-flap system can cause significant noise generation (refs. 1 to 6). These tests have also shown that the greater the exhaust gas velocity at or near the lifting surface, the greater the noise increase. Engines having low or moderate exhaust velocities are therefore more desirable for this application. However, these engines are generally larger and less efficient than the higher-pressure-ratio designs. Consequently, there has been an interest in nozzles that have geometric characteristics that cause rapid decay of the exhaust velocity and can be used with the higher-pressure-ratio fan engines. Nozzles having these characteristics have been designed and tested and are discussed in references 7 to 11.

In an attempt to demonstrate the full-scale practicality of a velocity-decayer nozzle and also to assess the associated acoustic and performance characteristics with a real engine, a 12-lobe nozzle (ref. 12) designed for rapid exhaust deceleration was fabricated and tested with an acoustically suppressed TF-34 turbofan engine (refs. 13 and 14). A mixed-flow cycle was used, with the engine core gas being discharged internally upstream of the nozzle exit. Tests were made with the engine alone and with the exhaust blowing at a wing-flap segment (ref. 15). This report presents the performance and acoustic characteristics of the engine and nozzle without the wing-flap segment.

APPARATUS AND PROCEDURE

Engine

The TF-34 turbofan engine is a dual-rotor front-fan configuration with a nominal bypass ratio of 6.5. It has a single-stage fan with a pressure ratio of 1.5 and a 14-stage axial-flow compressor with variable stators and a nominal pressure ratio of 14.5. The combustor is an annular type. The gas generator high-pressure turbine has two axial-flow stages, both air cooled. The fan low-pressure turbine has four axial-flow stages and drives the fan through a concentric shaft extending forward inside the gas generator rotor. Air is introduced directly to the fan rotor with no fan inlet guide vanes. A schematic of the engine is shown in figure 1.

Nacelle

An acoustically treated ground-test nacelle was designed (ref. 13), fabricated, and tested with a TF-34 engine. The results are reported in reference 14. The same nacelle was used in this test series and is shown in figure 2. The inlet consisted of a bellmouth attached to a cylindrical section housing three splitters. The splitters and the walls of the inlet had acoustic treatment consisting of perforated sheet over honeycomb.

The main nacelle consisted of the fan exhaust duct and the core engine cowling. The fan duct walls as well as the two fan duct splitters were acoustically treated with perforated face sheet over various thicknesses of a polyurethane open-cell foam (Scottfelt 3-900). A main support pylon on top and a narrow pylon on the bottom split the fan duct passage. The core exhaust system consisted of an annular duct lined with two thicknesses of a bulk suppression material (Cerafelt CR-400) held in place by wire screen and a perforated face sheet. In addition to the internal acoustic treatment, several layers of polyurethane foam and a vinyl-lead blanket were wrapped around the outer fan case.

Nozzles

The nozzle configurations investigated had a mixed exhaust, with the engine core gas discharged internally approximately 1 equivalent nozzle diameter upstream of the exit. Both an annular and a daisy-shaped core mixer nozzle were tested in conjunction with a daisy-shaped outer nozzle. Details of the daisy core mixer are shown in fig-

ure 3, and the hardware is shown in figure 4. The mixer forms a smooth transition from the 1810-square-centimeter (281-in^2) annular passage at the mixer entrance to 12 symmetric lobes around the centerbody that have a physical exit area of 1610 square centimeters (250 in^2). The annular core nozzle is a short cylindrical extension terminating at the same location as the entrance to the mixer. The exit area of the annular nozzle was 1810 square centimeters (281 in^2).

Details of the decayer nozzle for the mixed fan and core flow are shown in figure 5. The basis for the design is outlined in reference 12. The outer nozzle cowling was circular behind the fan duct splitter rings and transitioned into a 12-lobe daisy-shaped decayer at the exit. Briefly, the number of lobes, their shape and spacing, and the length of the decayer were a compromise between achieving the desired velocity decay and minimizing weight and performance loss. The 12-lobe decayer was symmetric except for the "3 o'clock" lobe, which was trimmed to a smaller radius to enable closer placement to a wing surface. Aerodynamically shaped inserts were used for modifying the exit area of the decayer from 6770 square centimeters (1050 in^2) to 5980 square centimeters (927 in^2). The lobes of the decayer were oriented in line with the lobes of the core mixer. A 20.4-centimeter (8.0-in.) radius centerbody extended aft from the turbine and closed with a low-angle plug downstream of the decayer exit. Turbine cooling air was discharged through a 4.6-centimeter (1.8-in.) diameter hole in the plug tip. The installed decayer nozzle is shown in figure 6.

Three nozzle configurations were tested: mixer core with large decayer; annular core with large decayer; and annular core with small decayer. The three nozzle configurations are shown schematically in figure 7.

Test Facility

The test facility is located on the edge of Rogers Dry Lake at Edwards Air Force Base. A gallows structure supported the engine above a steel base plate (fig. 6(b)). This plate was suspended by four flexure plates located below ground level. Thrust was measured at the forward end of the base plate by a load cell.

The engine was mounted with its horizontal centerline 2.75 meters (9 ft) above a flat concrete and steel surface. There were no major obstacles blocking the lines of sight between the engine and the various microphones. This test facility is at an altitude 700 meters (2300 ft) above sea level.

Instrumentation

Far-field acoustic data were recorded by 17 microphones spaced every 10 degrees from 0° to 160° on the arc of a 30.5-meter (100-ft) radius (fig. 8(a)). The center of the arc lay in the center of the exhaust nozzle exit plane. Zero degrees was taken from the engine centerline in front of the engine, counterclockwise looking down from above. The microphones were in the same horizontal plane as the engine centerline.

The locations of the various engine instrumentation stations are shown in figure 8(b). Total airflow was calculated from pressure and temperature measurements along with the known flow area at the bellmouth throat (station 1). Similar measurements taken at the core inlet (station 2c) were used to calculate core flow. Four five-element rakes at station 2 and eight five-element total pressure rakes behind the fan (station 24) were used to determine fan pressure ratio. Speed sensors were used to measure fan and core speeds. Engine instrumentation was also located at the core compressor outlet (station 3) and at the entrance (station 5.4) and outlet (station 6) of the low-pressure turbine. Pressure surveys were made behind the fan duct splitters (station 25) and in the core duct passage aft of the treatment (station 7). All survey rakes in the inlet and in the fan and core exit passages were removed when far-field acoustic measurements were made. More details of the instrumentation are presented in reference 14.

The ambient conditions (wind velocity, temperature, pressure, and relative humidity) were measured. Exhaust wake surveys were made with a portable 122-centimeter (48-in.) long rake. Twenty-four combination total pressure and temperature probes were located every 5.1 centimeters (2 in.). Between the combination probes were 24 static pressure elements. The rake was located behind the decayer nozzle (fig. 9).

Test Procedure

Tests were not started unless the wind speed was under 2.2 meters per second (5 mph) and were stopped if the wind speed exceeded 3.1 meters per second (7 mph). The engine was allowed to stabilize for 2 minutes at each power setting before data were taken. Acoustic tests were run between 3 a.m. and 8 a.m. because wind and background noise were low at these hours.

For far-field acoustic tests, the engine was run at five different power settings covering the range from maximum power to approximately half power. The maximum power setting corresponds to a maximum $T_{5.4}$ of 1085 K (1955° R), and the corresponding maximum fan speed was allowed to vary with ambient temperature. The

other four power settings correspond to physical fan speeds of 6500, 6200, 5800, and 5100 rpm.

During engine performance runs, nine or more power settings were recorded. Except for maximum power, these points were set by corrected fan speed.

RESULTS AND DISCUSSION

Acoustics

Acoustic characteristics are presented in figures 10 to 21, inclusive. The figures present overall sound pressure levels, perceived noise levels, selected sound pressure spectra at angles of 50°, 80°, 110°, and 130° from the inlet, and sound power spectra for each configuration over a range of power settings (corrected fan speeds). In general, although there were no large differences in the characteristics of the three configurations, the internal mixer did appear to cause a 1- to 2-decibel reduction in noise, and the reduction in decayer exit area did increase noise levels by 3 to 4 decibels.

Overall sound pressure levels (OASPL) at a 30.5-meter (100-ft) radius for the three nozzle configurations are presented in figures 10, 14, and 18. All configurations had a peak noise level in the aft quadrant (140° from the inlet) and a minimum level in the forward quadrant. Of the three nozzles, slightly higher noise levels were measured for the annular core with small decayer nozzle at a comparable corrected fan speed.

Larger differences than those among the OASPL values are seen in a perceived noise level (PNL) comparison along a 152.4-meter (500-ft) sideline (figs. 11, 15, and 19). The maximum PNL generally occurred 110° from the inlet for all the nozzles and fan speeds tested. The mixer core with large decayer was the quietest, while the annular core with large decayer and the annular core with small decayer were about 1 and 4 decibels louder, respectively.

One-third-octave spectra along a 152.4-meter (500-ft) sideline for the three nozzles tested at selected angles of 50°, 80°, 110°, and 130° from the inlet are presented in figures 12, 16, and 20. At 110° the mixer core with large decayer had slightly lower sound pressure levels (SPL) above 500 hertz than did the other two configurations. Comparison of the spectra at 130° from the inlet reveals a sharp rolloff in SPL occurring at 2500 hertz for the mixer core with large decayer. The annular core with large decayer and the annular core with small decayer have sharp rolloffs in the spectra at 3150 and 4000 hertz, respectively.

Only small differences in sound power spectra for the three configurations can be

seen in figures 13, 17, and 21. At comparable corrected fan speeds, power levels above about 400 hertz were greatest for the annular core with small decayer and least for the mixer core with large decayer. All configurations had a peak in the power spectra at 630 hertz.

A spectral comparison of the mixer core with large decayer nozzle is made with the coannular exhaust nozzle in figure 22. As mentioned previously, all the decayers had similar spectra. Although the sound pressure level of the decayer was considerably lower at the low frequencies, it was significantly higher than the coannular SPL above 315 hertz, where the annoyance factor is greater. The shift in the frequencies at which the peak SPL's occurred for the coannular and decayer nozzles was about a factor of 10; and it was inversely proportional to the ratio of the characteristic dimensions of the two nozzle geometries. The effective diameter of the coannular nozzle was 94 centimeters (37.0 in.), and the slot height of the lobe of the decayer nozzle was 9.4 centimeters (3.7 in.).

Aerodynamic Performance

The aerodynamic performance characteristics of the quieted engine with the three mixed velocity-decayer configurations are compared with those from a separate-flow coannular configuration of the same engine (ref. 14) in figure 23. The separate-flow configuration had a coannular nozzle with core and fan exhaust exit areas of 1810 square centimeters (280 in^2) and 5100 square centimeters (790 in^2), respectively. The same nacelle acoustic treatment was used in all the tests.

Figure 23(a) presents corrected fan speed as a function of the high-pressure-turbine discharge temperature. Engine performance was rated at a $T_{5.4}$ of 1085 K (1955° R). It can be seen that the fan speeds were from 2 to 4 percent lower for the decayer configurations than for the coannular nozzle. Airflow characteristics for the two large-area decayer nozzles were identical and slightly higher than for the coannular nozzle (fig. 23(b)). However, the small-area decayer had the lowest airflow. The reduced airflow coupled with the highest fan pressure ratio (fig. 23(c)) indicated a shift in operating point due to backpressuring of the fan stage for the small-area decayer. The large-area decayer configurations had fan pressure ratio characteristics identical to those of the coannular nozzle.

Corrected thrust is presented as a function of turbine discharge temperature and corrected fan speed in figures 23(d) and (e), respectively. At comparable $T_{5.4}$ (fig. 23(d)), the thrust levels were identical for the three decayer configurations but were about 6 percent lower than that of the coannular configuration. However, when compared on a fan speed basis (fig. 23(e)), the small-decayer configuration had thrust

levels several percent higher than the large-decayer and coannular configurations.

Bypass ratio as a function of fan speed is presented in figure 23(f). At rated fan speed, the small-area decayer had a fan- to core-airflow ratio of 6.1 as compared with 6.5 for the large-area decayer configurations and 6.7 for the coannular configuration. No significant differences were measured in specific fuel consumptions for the decayer configurations (fig. 23(g)), but they were 5 to 8 percent greater than for the coannular configuration over the range of fan speeds tested.

Figure 24 presents fan and core flow velocities for the three test configurations and the coannular nozzle. Velocities were calculated from measured gas properties at stations 25 and 7 and the assumption of isentropic expansion to ambient static pressure. Significant backpressuring of the core flow with the decayer nozzles is evident, with core velocities 40 to 60 percent greater than those obtained with the coannular nozzle. However, the fan velocities are similar for all the configurations.

In an attempt to correlate jet noise, an effective velocity parameter was calculated, where

$$\overline{V} = \sqrt[8]{\frac{V_f^8 + V_c^8 \frac{A_c}{A_f}}{1 + \frac{A_c}{A_f}}} \tag{1}$$

and $A_c/A_f = 0.313$, 0.366, and 0.435, respectively, for the mixer-core-with-large-decayer, annular-core-with-large-decayer, and annular-core-with-small-decayer configurations. The effective velocities are presented as a function of corrected fan speed and thrust in figures 25(a) and (b), respectively. It can be seen that the effective velocity of the decayer nozzles was considerably greater than that of the coannular nozzle over the entire range of power settings tested. The small-area decayer had the highest velocities of the decayers tested.

An attempt was made to arrive at the thrust loss associated with the nozzle assemblies tested. The measured thrust of the engine-nozzle assembly was ratioed to the sum of the ideal momentum of the fan and core streams calculated from gas properties and weight flows at stations 25 and 7, respectively. The thrust coefficient obtained in this manner is shown in figure 26. The total nozzle losses were of the order of 4 percent greater for the decayer configurations than for the separate-flow coannular exhaust system (ref. 14), which was calculated in a similar manner. This thrust loss was due to additional wall friction (estimated to be ~1 percent), core and fan flow mixing losses, exit flow angularity, and base pressure forces on the outer surfaces of the decayer.

Exhaust Surveys

Exhaust velocities were calculated from total pressure, static pressure, and total temperature measurements made with the survey rake and from isentropic gas dynamic relations. The rake was located in three positions with respect to the engine centerline, as shown in figure 27. Complete velocity profiles are reported for rake position A, directly behind a lobe and the centerbody. Rake positions B and C were used to provide three data points each for the velocity level at locations close to the exit plane (0.03 m (1 in.) from the exit). Rake data at position A were taken at five axial locations for the annular core with large decayer and for the annular core with small decayer. However, only two axial locations were used for the mixer core with large decayer.

Velocity profiles. - Visual as well as rake survey data indicated the core flow to have a significantly large radial component at the decayer exit. Figure 28 schematically shows the velocity profiles and flow lines behind a typical lobe near the exit for a high power setting. A region of local flow separation appeared to exist at the inner portion of the lobes and the engine centerbody. This flow pattern existed for all the configurations tested.

Figures 29 to 31, inclusive, show the measured velocity profiles directly behind the lobe for the three nozzle assemblies. The variation in profile shape with axial distance from the decayer exit is generally similar for all three nozzles. There is a continued tendency for a radially outward movement of the outer boundary of the plume in all cases, with an essentially uniform velocity at the largest distance.

Decay rates. - All decayer configurations had significantly faster exhaust-flow mixing than did the coannular configuration. Peak exhaust gas temperature variation is presented in figure 32. The internal mixer appeared to be more effective than the annular core in mixing the hot gas close to the exit. However, little difference was measured 4.6 meters (181 in.) from the exit.

Peak exhaust velocity is presented at various locations from the nozzle, in absolute distance, in figure 33 for the rated speed case. The original design variation (from ref. 12) is also shown. The trends are similar for all three decayer configurations. Immediately behind the nozzle, the peak velocity for the decayer configurations was very nearly equal to the calculated exhaust velocity of the core flow (solid symbols, fig. 24), indicating no measurable internal mixing. The decay of the actual velocity was considerably greater than the design variation near the nozzle exit. At distances corresponding to the flap location (~120 to 160 in.), the actual velocity was about 25 percent lower than the design value.

Exhaust velocity decay in terms of nondimensional parameters is shown in figure 34. Equivalent diameter D_e is defined as the diameter of a circle of area equal

to the total exit area of each of the decayers tested. As in the previous figure, all decayer configurations had velocity decay greater than the design values. At 3 equivalent nozzle diameters from the nozzle exit, the velocity decayed to approximately 0.35 of the maximum value at the nozzle exit. The observed rapid decay was probably due largely to the unmixed flow field and large decayer core-flow radial component in the exit plane of the decayer nozzles (e.g., fig. 28).

Comparisons of Acoustic and Aerodynamic Performance Results

The maximum perceived sideline noise levels of the three mixer velocity-decayer nozzle configurations are compared with the separate flow-coannular nozzle configuration (ref. 14) as a function of corrected thrust in figure 35. As can be seen, the mixer velocity-decayer configurations were considerably noisier (8 to 11 PNdB) at comparable thrust levels than the separate-flow configuration. The installation containing the mixer core was approximately 2 PNdB quieter at the higher thrust levels than the one with the annular core and the same large decayer. However, the exhaust velocities of the decayer nozzle assemblies were substantially higher than the exhaust velocity of the coannular nozzle at the same thrust level (fig. 25).

An attempt was made to correlate noise levels with an area-weighted effective exhaust velocity $\overline{V}$, assuming an eighth-power velocity dependence (eq. (1)). Overall sound power level (PWL), peak overall sound pressure level (OASPL) on a 30.5-meter (100-ft) radius, and peak perceived noise level (PNL) on 152.4-meter (500-ft) sideline are presented as functions of the calculated effective velocity in figure 36. All noise levels were normalized with respect to the nozzle exit area. The separate-flow coannular configuration is also presented.

The sound power and sound pressure level data were quite similar for all the configurations tested and slightly less than for the coannular configuration. However, the perceived noise level along a 152.4-meter (500-ft) sideline for the internal mixer configuration was about 2 decibels lower than for the other decayer installations, but all were from 1 to 4 decibels louder than the coannular configuration. The increase in PNL as compared with the coannular configuration was the result of the frequency shift of the sound pressure spectra with the decayer nozzles (fig. 22).

In interpreting the results shown in figure 36, note that the effective exhaust velocity $\overline{V}$ as obtained by equation (1) is based on ideal expansion values (nozzle velocity coefficient of 1). However, in view of the approximately 4 percent difference in nozzle thrust coefficients (fig. 26), the effective velocity for the decayer nozzles in figure 36 should be reduced by about 2 percent relative to the effective velocity of the coannular nozzle. Such an adjustment would produce equal OASPL's, very nearly equal PWL's,

and an increase in PNL of about 2 to 5 PNdB. The velocity adjustment would also tend to produce the same slopes for the noise-velocity variations of the decayer and coannular nozzle configurations. The effective velocity dependence of the acoustic data in this case would be close to the seventh power.

Although it is not certain that an eighth-power area-averaged velocity is the correct effective velocity for correlating the noise data, it is apparent from the preceding discussions that the measured noise is predominantly jet noise. The resultant perceived noise levels will therefore depend primarily on the exhaust velocity of the nozzle and the geometry of the nozzle configuration (effect on frequency of spectrum peak).

CONCLUDING REMARKS

In considering the results of these tests for application to externally blown flap systems, note that reductions in the flap impingement velocity required to reduce flap-generated noise (by 10 to 15 PNdB) are no greater than approximately 100 meters per second (305 ft/sec). The decayer nozzle configurations tested were therefore overdesigned, in that peak velocity reductions of the order of 230 to 250 meters per second (750 to 830 ft/sec) were obtained at 3 to 5 equivalent nozzle diameters, respectively. Furthermore, the nozzle configurations backpressured the engine such that the core discharge velocities were increased substantially over that for a separate-flow coannular nozzle tested on the same engine. The increased nozzle velocity for the decayer configurations could have unnecessarily increased both the nozzle thrust loss and the jet noise level.

A revised decayer nozzle could probably be designed for a more moderate decay rate (of the order of 100 m/sec (305 ft/sec) at 4 equivalent diameters) and enlarged discharge area (no engine backpressure) with considerably less thrust loss. A design with fewer lobes of lower aspect ratio and better aerodynamic contours would contribute much to reduce internal losses. A revised lobe design would also reduce the peak frequency shift to minimize the effect on perceived noise. When considering that the decayer nozzles tested showed essentially no change in sound power level as compared with the coannular nozzle (based on calculated effective exhaust velocity), it is conceivable that a modified decayer design that maintains the design exhaust velocity level might have a significantly improved noise characteristic. It should therefore be possible to obtain an optimum decayer design for reducing flap noise with small thrust loss and very little, if any, noise penalty.

SUMMARY OF RESULTS

Static tests were made on a quieted TF-34 turbofan with a 12-lobe exhaust nozzle designed for rapid velocity decay. The engine core flow was discharged internally approximately 1 equivalent nozzle diameter upstream of the exit. Both an annular and a daisy-shaped core nozzle were tested. Tests with the annular core nozzle were made with two decayer exit areas. Far-field acoustic, aerodynamic performance, and wake survey measurements were made; and results were compared with those obtained with a separate-flow coannular nozzle tested on the same engine. A summary of the results follows:

1. Along a 30.5-meter (100-ft) radius from the exit, sound pressure level peaked 140° from the inlet; however, when extrapolated to a 152.4-meter (500-ft) sideline and converted to a perceived noise level, the peak occurred 110° from the inlet.

2. At comparable effective exhaust velocities, no difference in maximum overall sound pressure level was observed with the various configurations along a 30.5-meter (100-ft) radius; however, the maximum perceived noise level at a 152.4-meter (500-ft) sideline was reduced approximately 2 decibels with the use of an internal core mixer.

3. All decayer configurations had a pronounced spectrum shift to higher frequencies as compared with the separate-flow coannular nozzle. The peak sound pressure level occurred at a frequency inversely proportional to a characteristic dimension of the nozzles. This dimension appeared to be the slot height of a lobe for the decayer nozzles and the diameter of a circular nozzle of equivalent total exhaust area for the coannular configuration.

4. The increase in internal losses associated with the decayer nozzle configurations (as compared with the coannular nozzle) were equivalent to about 4 percent of the engine thrust.

5. All three decayer nozzle configurations produced a backpressure on the engine such that the effective exhaust velocities were substantially greater than those for the coannular nozzle at the same engine power setting. The increase in effective exhaust velocity was the primary cause of the higher noise levels of the decayer nozzles.

6. The degree of velocity decay appeared to be insensitive to whether or not an internal core mixer was used and to a 12 percent variation in decayer exit area.

7. The exhaust velocity decayed to 0.35 of its peak value, as compared with no decay for a separate-flow coannular nozzle, within 3 equivalent nozzle diameters of the exit. The peak exhaust gas temperature was 400 K (720° R) lower for the decayer nozzles at the same location. The measured decay rates for the decayer nozzles were substantially greater than the design values.

8. Along a 152.4-meter (500-ft) sideline, the decayer nozzles were approximately 2 to 4 decibels louder at comparable effective exhaust velocities and 8 to 11 decibels louder at comparable thrust levels than a separate-flow coannular nozzle. The decayer nozzle with the mixer core produced less perceived noise than did the other decayer configurations. Inasmuch as the variations in power level and maximum overall sound pressure level with effective velocity were essentially the same for the coannular and decayer nozzles, the increase in perceived noise level for the decayer nozzles was attributed to their spectrum frequency shifts.

Lewis Research Center,
National Aeronautics and Space Administration,
Cleveland, Ohio, April 15, 1976,
505-05.

APPENDIX - SYMBOLS

A area, m^2 (ft^2)

A_r reference area, 0.093 m^2 (1.0 ft^2)

C_T ratio of measured thrust to potential thrust

D_e diameter of an equivalent circular nozzle based on total nozzle area

F thrust, N (lbf)

N_f fan speed, rpm

P pressure, N/m^2 (psia)

T temperature, K (^oR)

V velocity, m/sec (ft/sec)

W airflow rate, kg/sec (lb/sec)

δ pressure correction factor, P/P_{ref}

θ temperature correction factor, T/T_{ref}

Subscripts:

c core

d decayer

f fan

n net

Note: Numerical subscripts refer to engine stations as defined in fig. 8(b).

Superscript:

$-$ effective

REFERENCES

1. Dorsch, R. G.; Krejsa, E. A.; and Olsen, W. A.: Blown Flap Noise Research. AIAA Paper 71-745, June 1971.

2. Dorsch, R. G.; Kreim, W. J.; Olsen, W. A.: Externally Blown Flap Noise. AIAA Paper 72-129, Jan. 1972.

3. Olsen, William A.; Dorsch, Robert G.; and Miles, Jeffrey H.: Noise Produced by a Small-Scale Externally Blown Flap. NASA TN D-6636, 1972.

4. Dorsch, Robert G.; et al.: Flap Noise. Aircraft Engine Noise Reduction, NASA SP-311, 1972, pp. 259-290.

5. Dorsch, R. G.; Goodykoontz, J. H.; and Sargent, N. B.: Effect of Configuration Variations on Externally Blown Flap Noise. AIAA Paper 74-190, Jan.-Feb. 1974.

6. Dorsch, R. G.: Externally Blown Flap Noise Research. SAE Paper 740468, Apr.-May 1974.

7. von Glahn, U. H.; Groesbeck, D. E.; and Huff, R. G.: Peak Axial-Velocity Decay with Single- and Multi-Element Nozzles. AIAA Paper 72-48, Jan. 1972.

8. Goodykoontz, Jack H.; Olsen, William A.; and Dorsch, Robert G.: Small-Scale Tests of the Mixer Nozzle Concept for Reducing Blown Flap Noise. NASA TM X-2638, 1972.

9. Goodykoontz, Jack H.; Dorsch, Robert G.; and Groesbeck, Donald E.: Noise Tests of a Mixer Nozzle - Externally Blown Flap System. NASA TN D-7236, 1973.

10. Goodykoontz, Jack H.; Wagner, Jack M.; and Sargent, Noel B.: Noise Measurements for Various Configurations of a Model of a Mixer Nozzle - Externally Blown Flap System. NASA TM X-2776, 1973.

11. Goodykoontz, J. H.; Dorsch, R. G.; and Wagner, J. M.: Acoustic Characteristics of Externally Blown Flap Systems with Mixer Nozzles. AIAA Paper 74-192, Jan.-Feb. 1974.

12. Chamay, A.; et al.: Design of a TF-34 Turbofan Mixer for Reduction of Flap Impingement Noise. (General Electric Co.; NAS3-14330), NASA CR-120916, 1972.

13. Edkins, D. P.: Acoustically Treated Ground Test Nacelle for the General Electric TF-34 Turbofan. (General Electric Co.; NAS3-14338), NASA CR-120915, 1972.

14. Jones, W. L.; Heidelberg, L. J.; and Goldman, R. G.: Highly Noise Suppressed Bypass 6 Engine for STOL Application. AIAA Paper 73-1031, Oct. 1973.

15. Samanich, N. E.; Heidelberg, L. J.; and Jones, W. L.: Effect of Exhaust Nozzle Configuration on Aerodynamic and Acoustic Performance of an Externally Blown Flap System with a Quiet 6:1 Bypass Ratio Engine. AIAA Paper 73-1217, Nov. 1973.

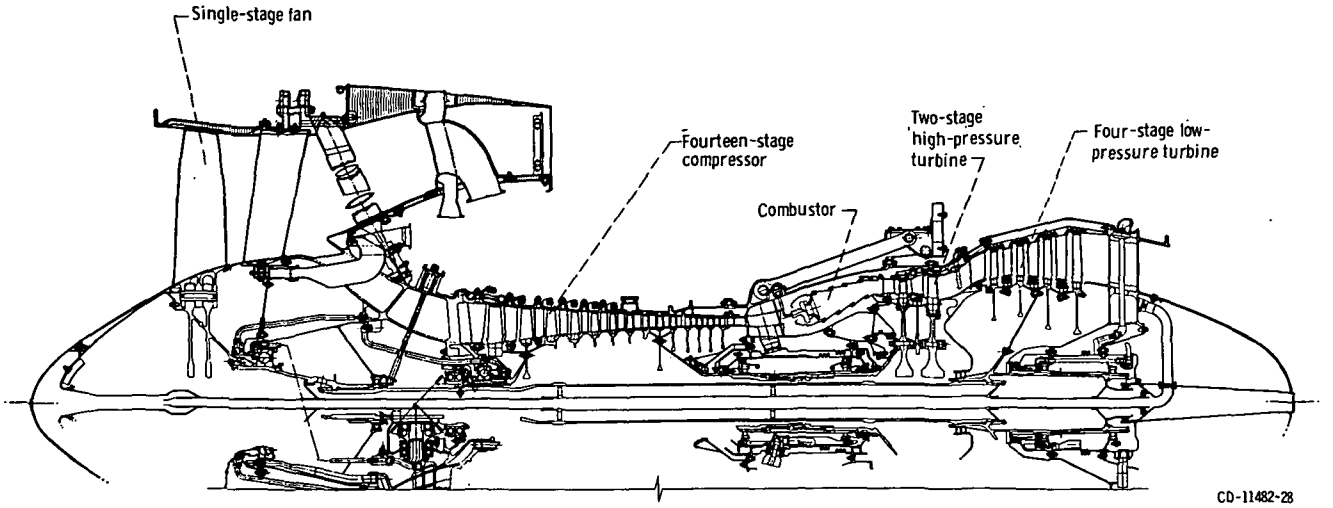

Figure 1. - Schematic of TF-34 turbofan engine.

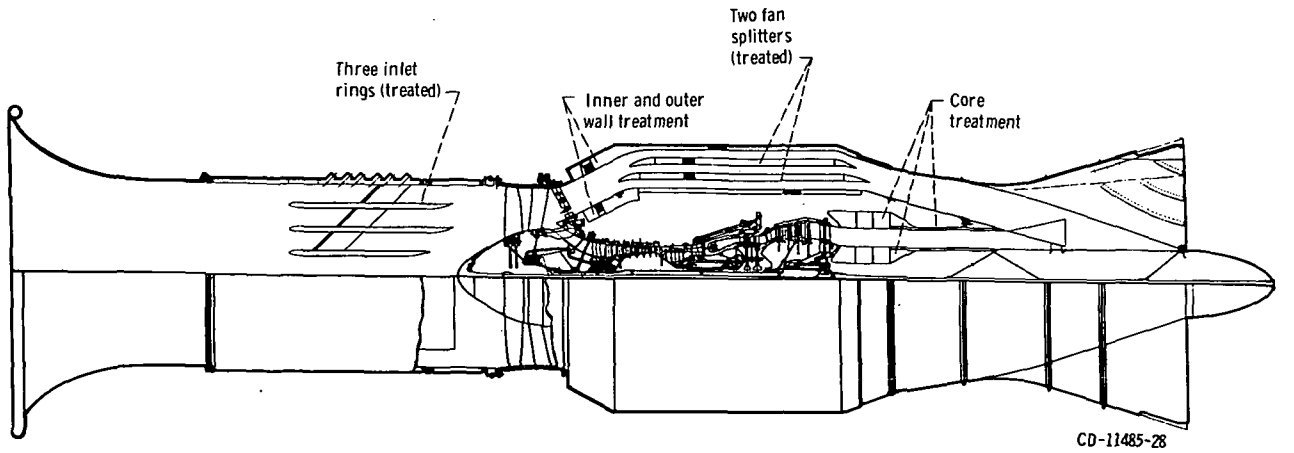

Figure 2. - Schematic of acoustically treated nacelle.

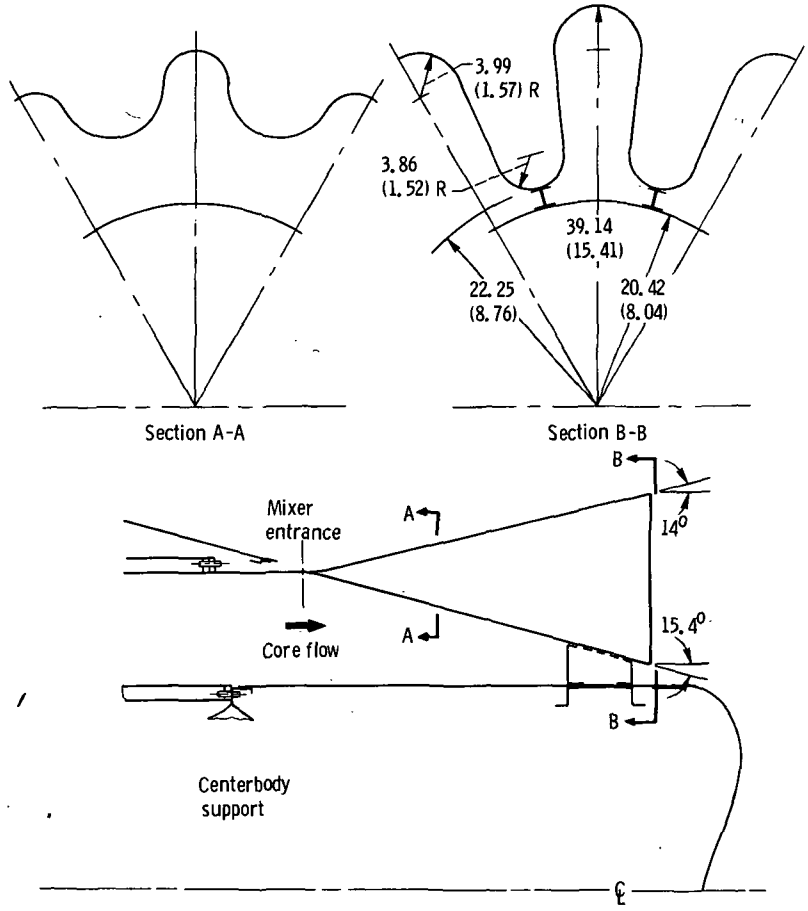

Figure 3. - Details of 12-lobe internal core mixer. (All dimensions are in cm (in.).)

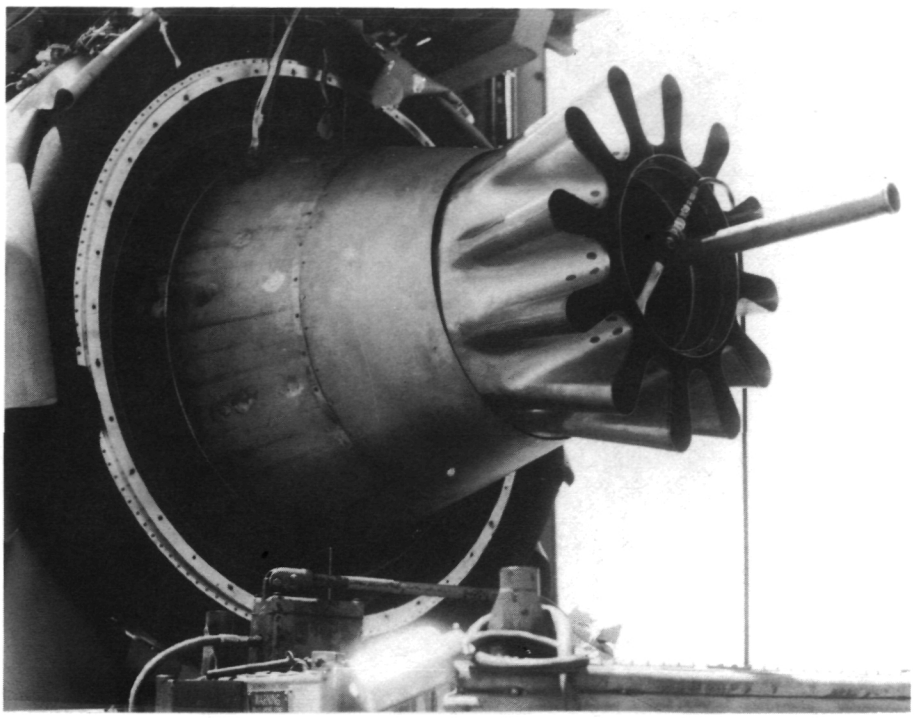

Figure 4. - Internal core mixer.

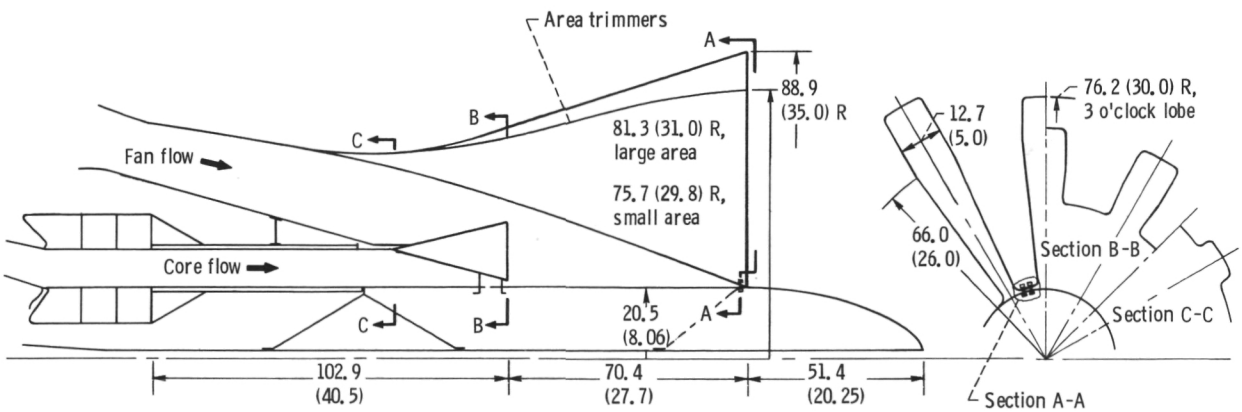

Figure 5. - Details of decayer nozzle. (All dimensions are in cm (in.).)

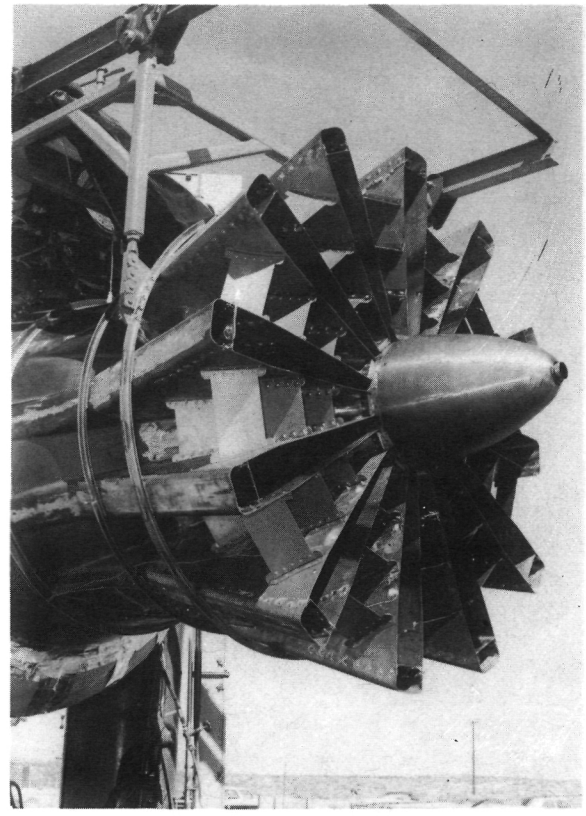

(a) Decayer nozzle.

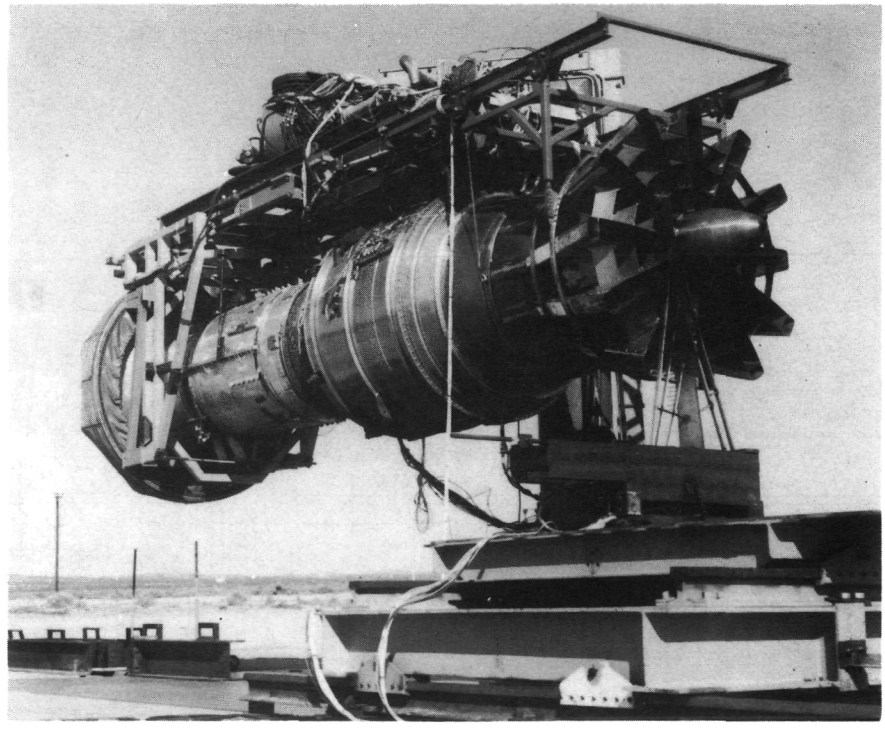

(b) Complete installation.

Figure 6. - Photograph of test hardware.

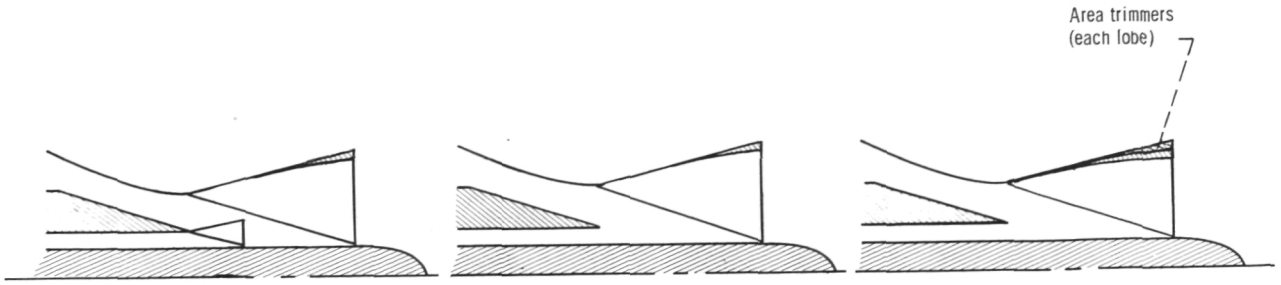

(a) Mixer core, 1610 square centimeters (250 in^2); and large decayer, 6770 square centimeters (1050 in^2).

(b) Annular core, 1810 square centimeters (281 in^2); and large decayer, 6770 square centimeters (1050 in^2).

(c) Annular core, 1810 square centimeters (281 in^2); and small decayer, 5980 square centimeters (927 in^2).

Figure 7. - Schematic of exhaust configurations tested.

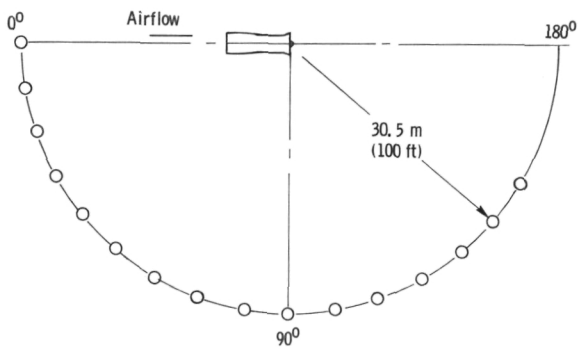

(a) Microphone arrangement (plan view).

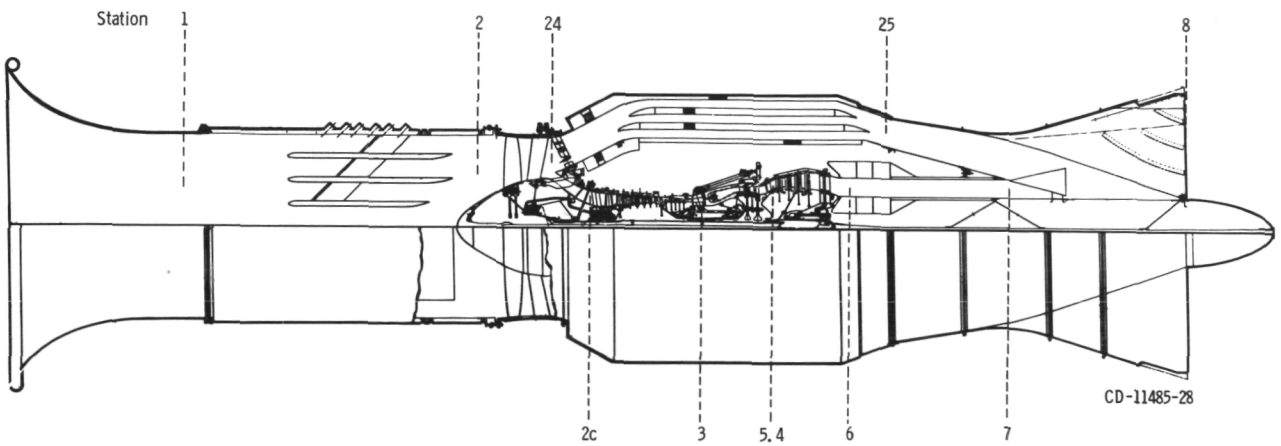

(b) Engine station designation.

Figure 8. - Instrumentation.

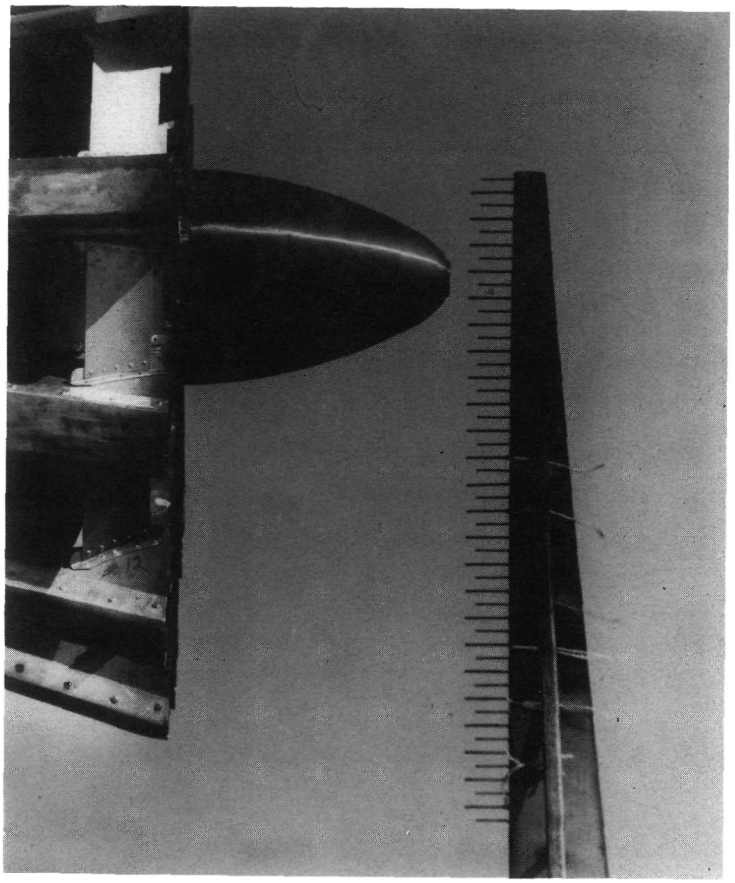

Figure 9. - Survey rake installed behind decayer nozzle.

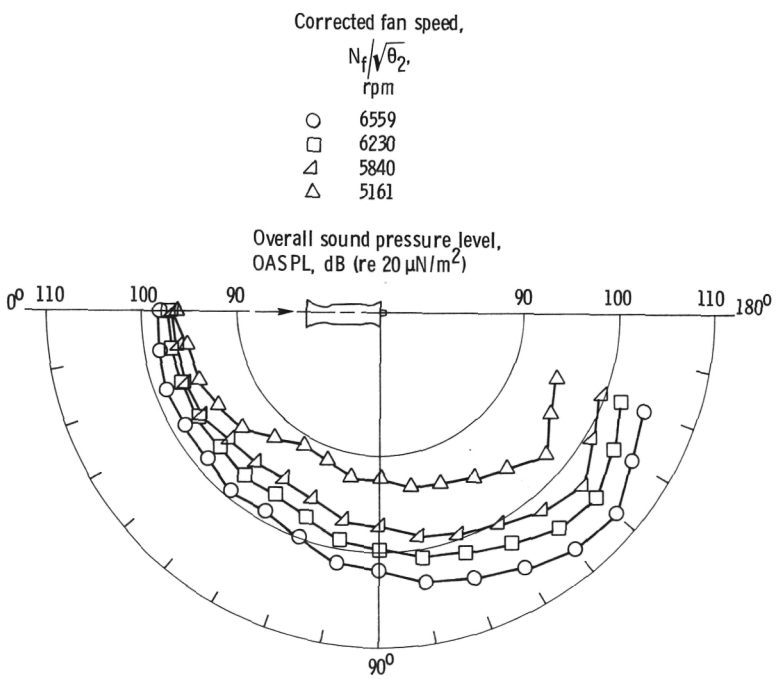

Figure 10. - Overall sound pressure level radiation at 30.5-meter (100-ft) radius of mixer core with large decayer nozzle.

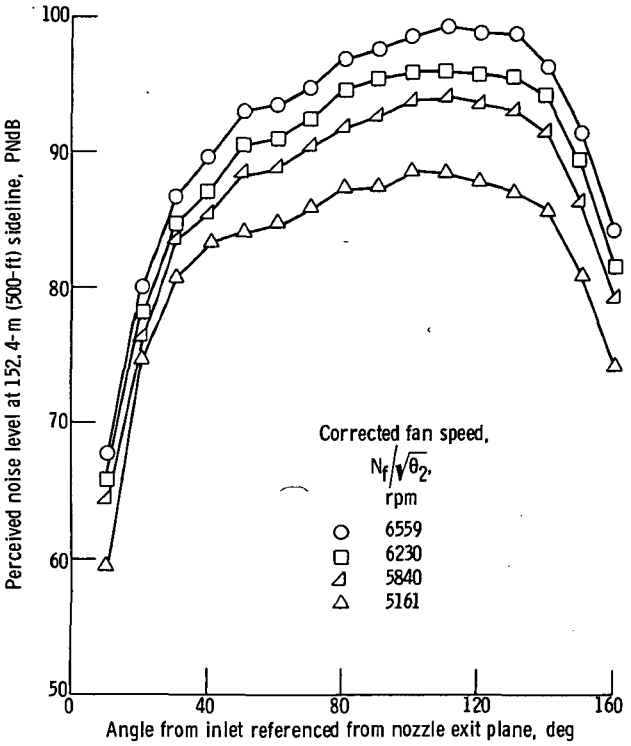

Figure 11. - Acoustic directivity characteristics of mixer core with large decayer nozzle.

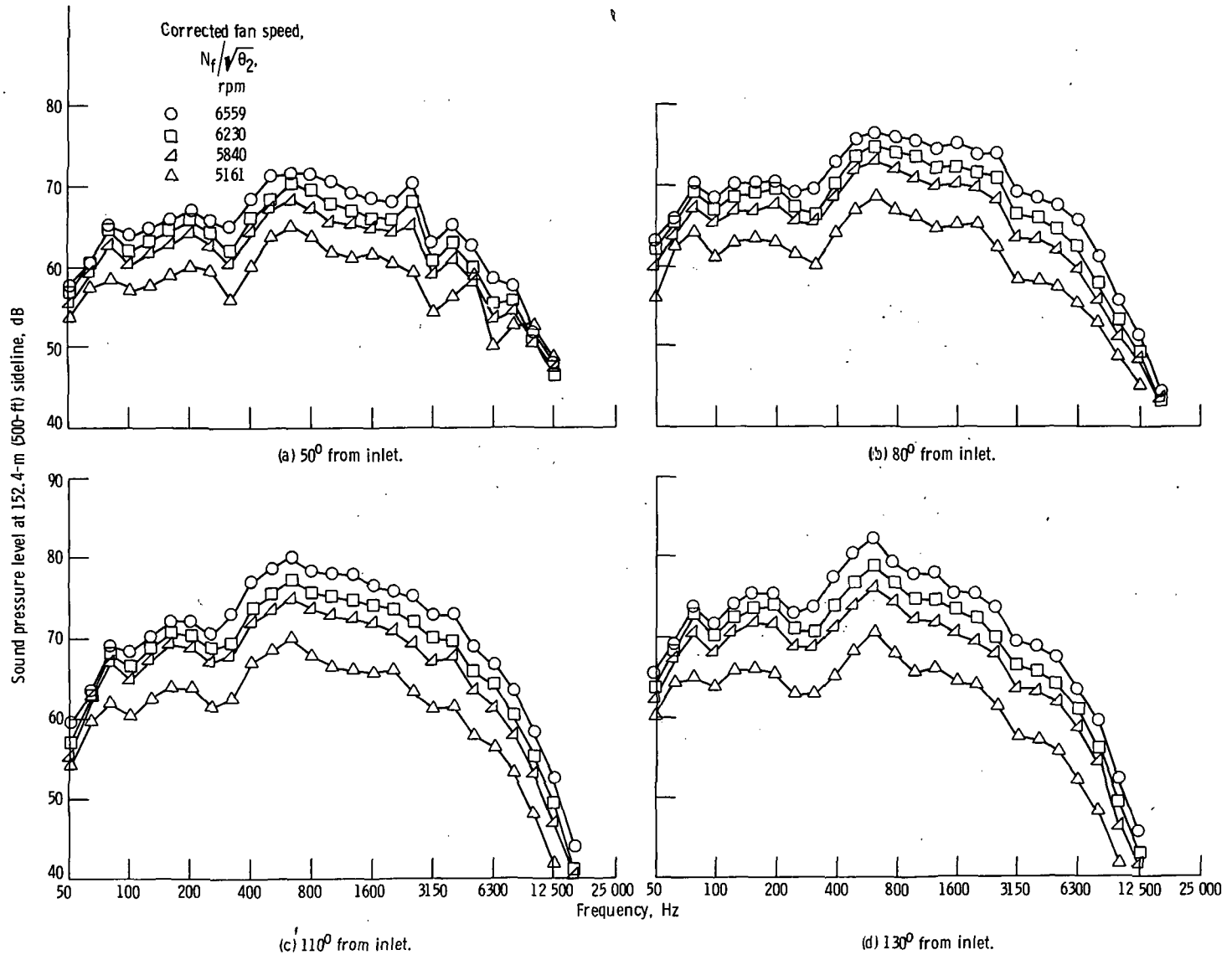

Figure 12. - Sideline 1/3-octave spectra of mixer core with large decayer nozzle.

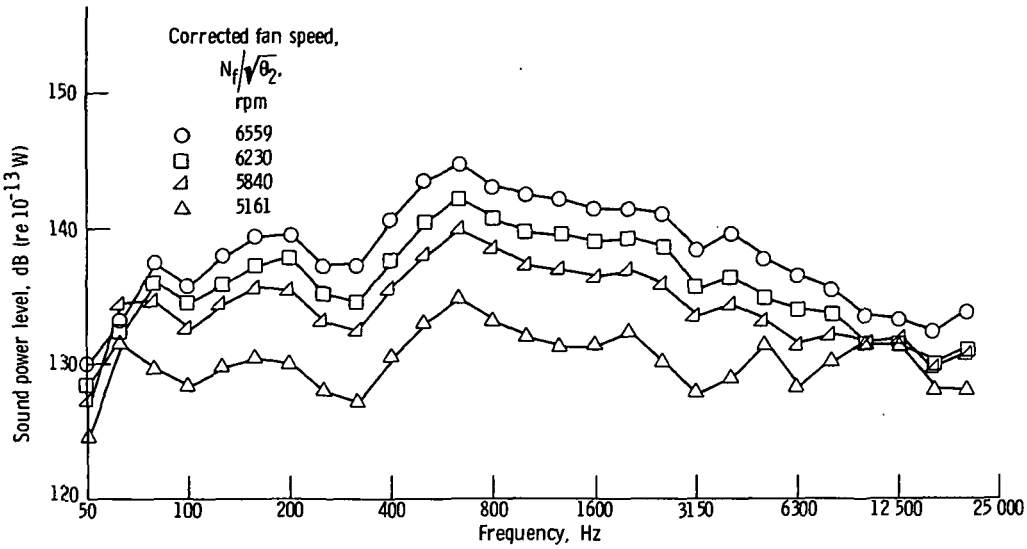

Figure 13. - Sound power spectra of mixer core with large decayer nozzle.

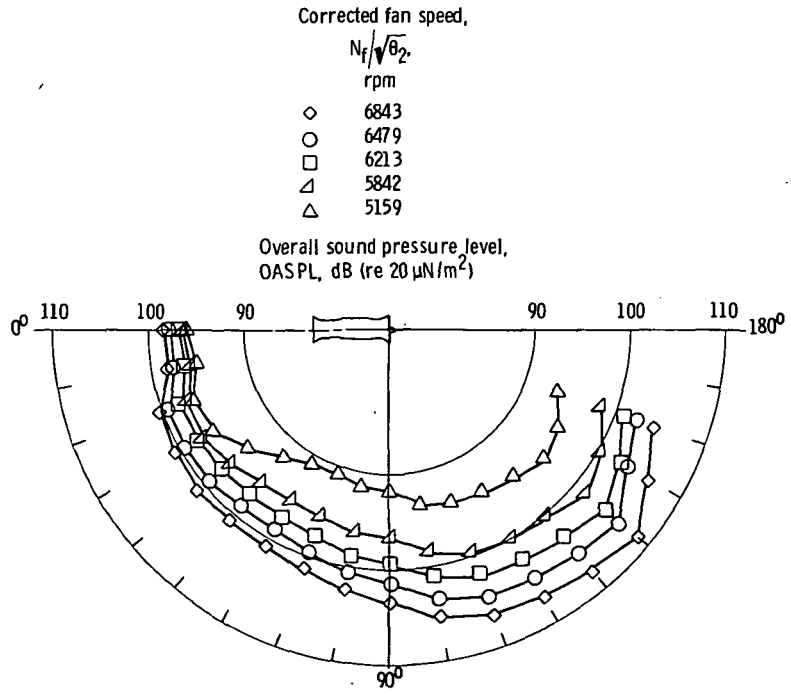

Figure 14. - Overall sound pressure level radiation at 30.5-meter (100-ft) radius for annular core with large decayer nozzle.

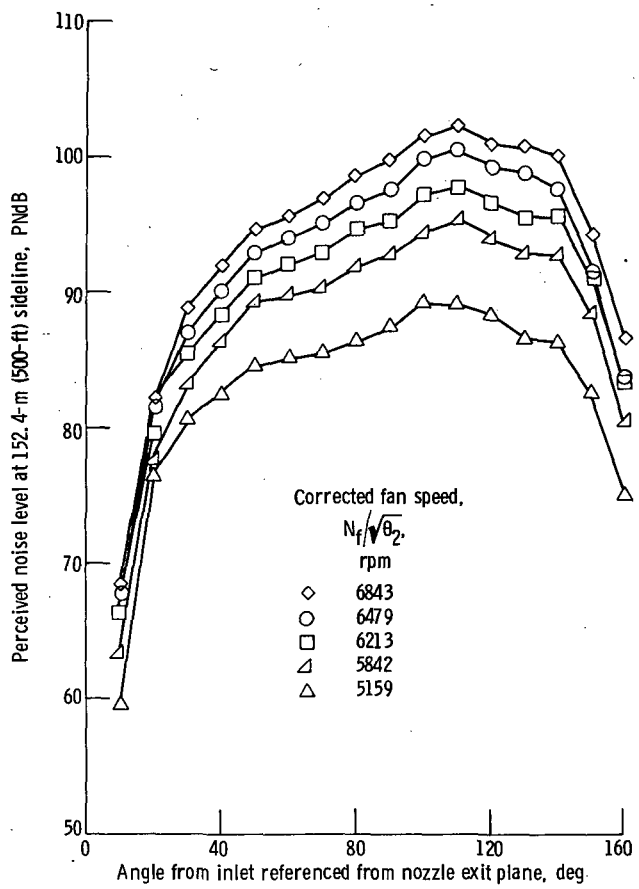

Figure 15. - Acoustic directivity characteristics of annular core with large decayer nozzle.

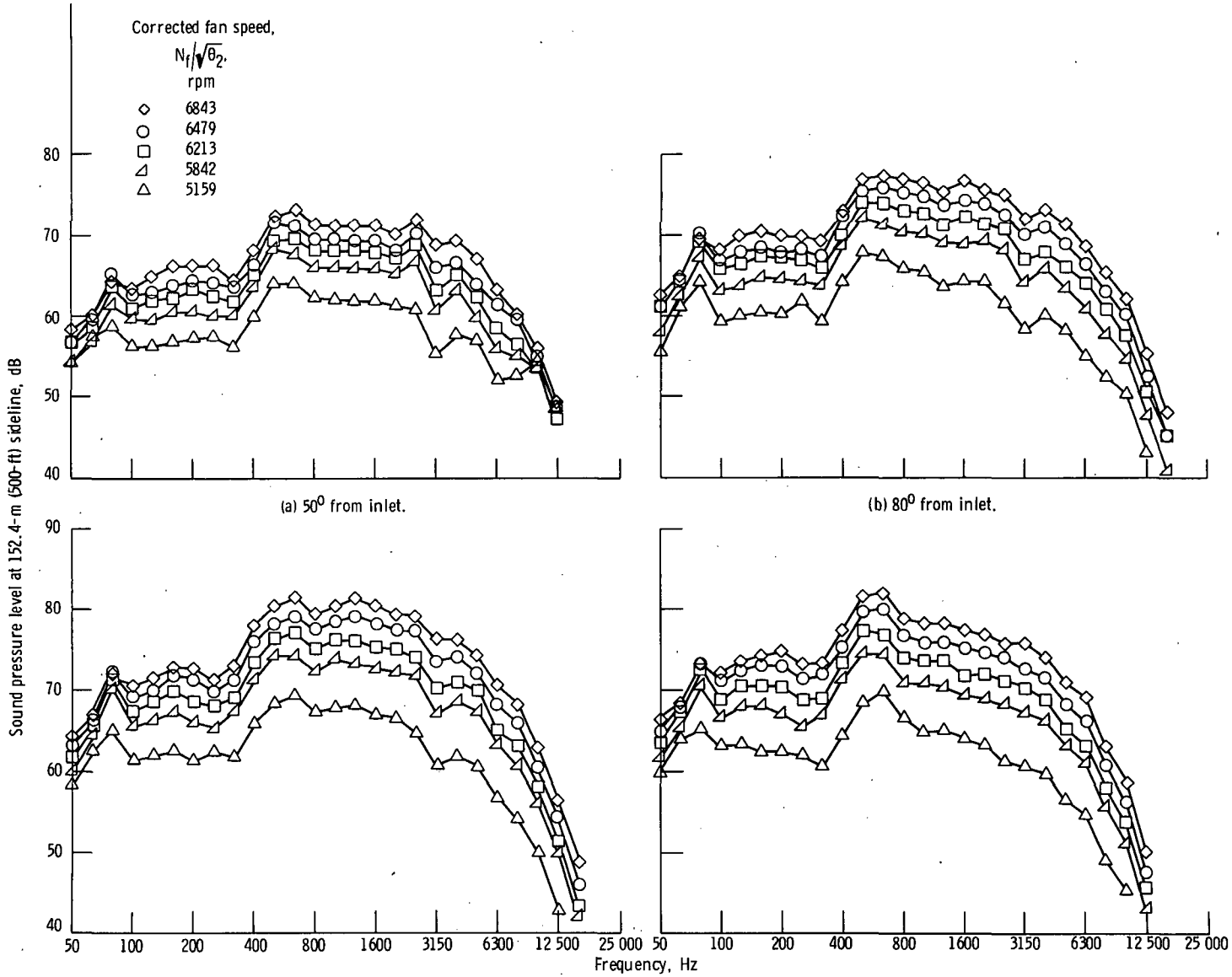

(a) 50^0 from inlet.

(b) 80^0 from inlet.

(c) 110^0 from inlet.

(d) 130^0 from inlet.

Figure 16. - Sideline 1/3-octave spectra of annular core with large decayer nozzle.

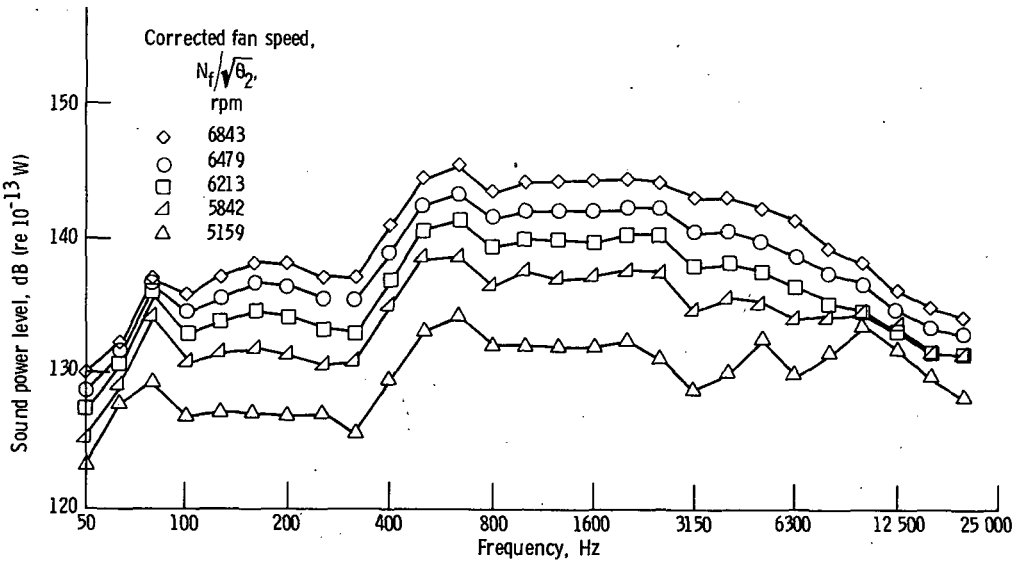

Figure 17. - Sound power spectra of annular core with large decayer.

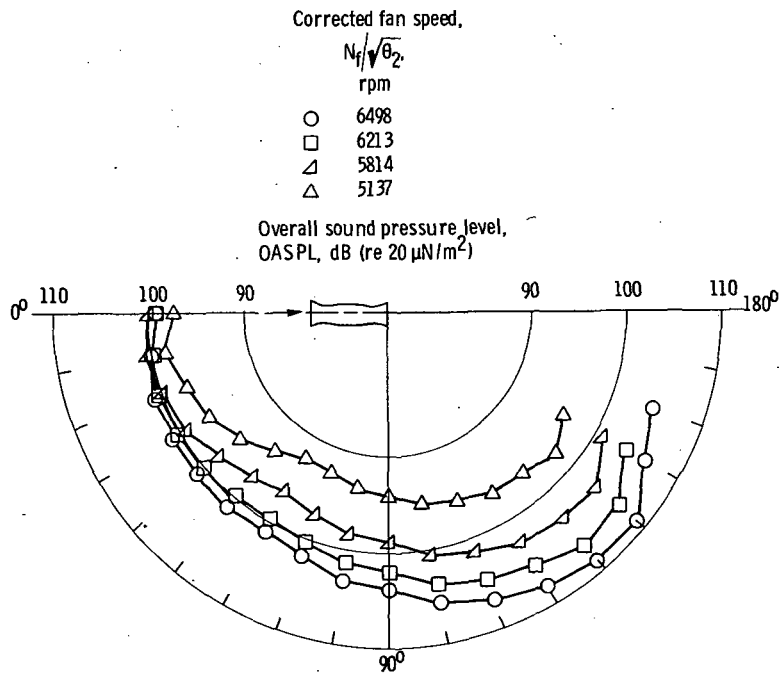

Figure 18. - Overall sound pressure level radiation at 30.5-meter (100-ft) radius for annular core with small decayer nozzle.

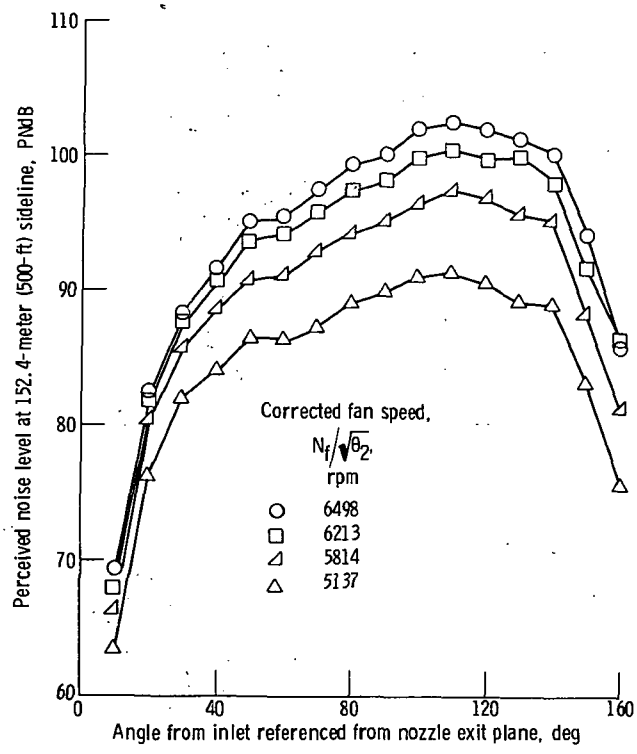

Figure 19. - Acoustic directivity characteristics of annular core with small decayer nozzle.

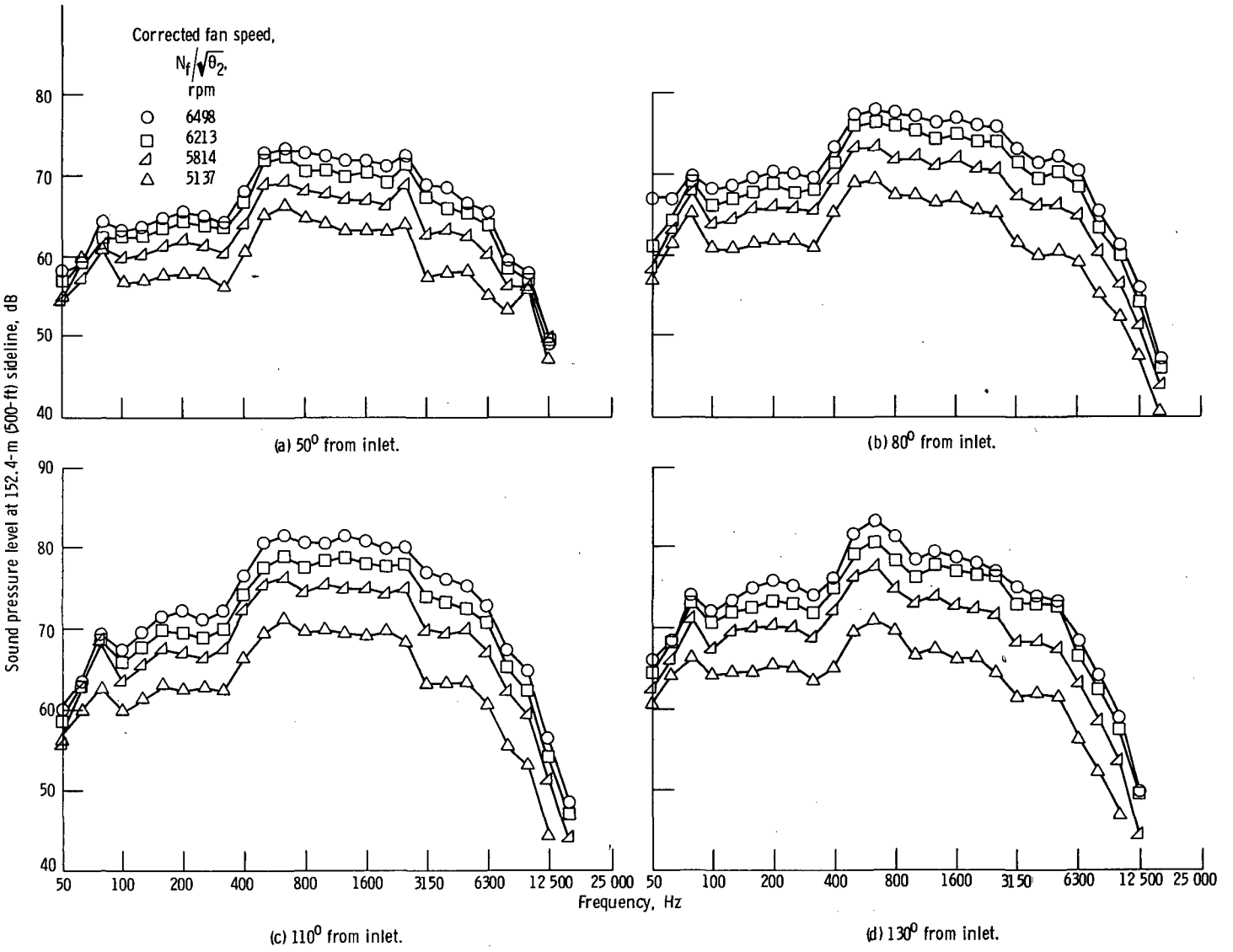

(a) 50^0 from inlet.

(b) 80^0 from inlet.

(c) 110^0 from inlet.

(d) 130^0 from inlet.

Figure 20. - Sideline 1/3-octave spectra of annular core with small decayer nozzle.

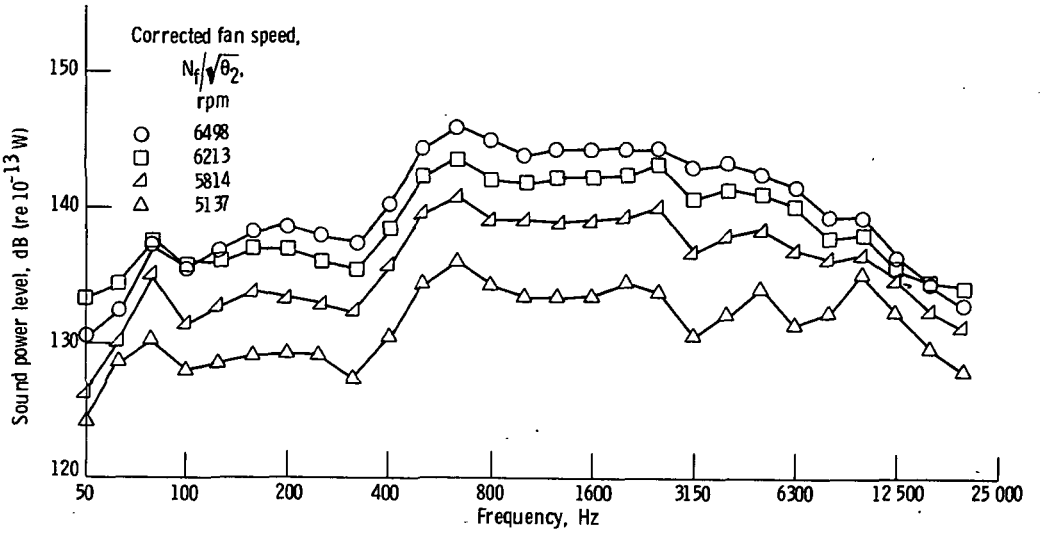

Figure 21. - Sound power spectra of annular core with small decayer nozzle.

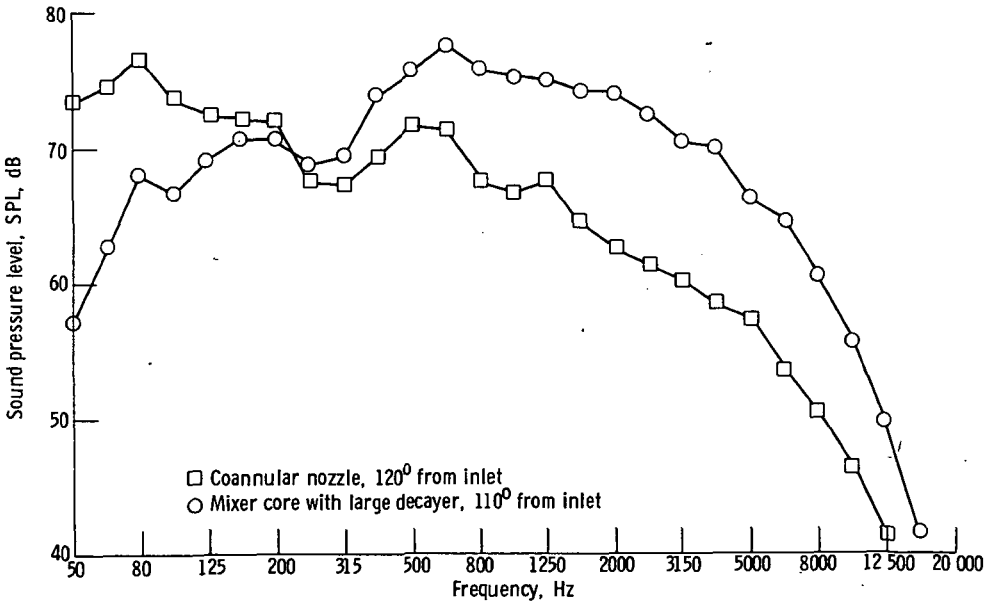

Figure 22. - 1/3-octave spectra at maximum perceived noise level on 152.4-meter (500-ft) sideline. Corrected fan speed, $N_f\sqrt{\theta_2}$, ~ 6270 rpm.

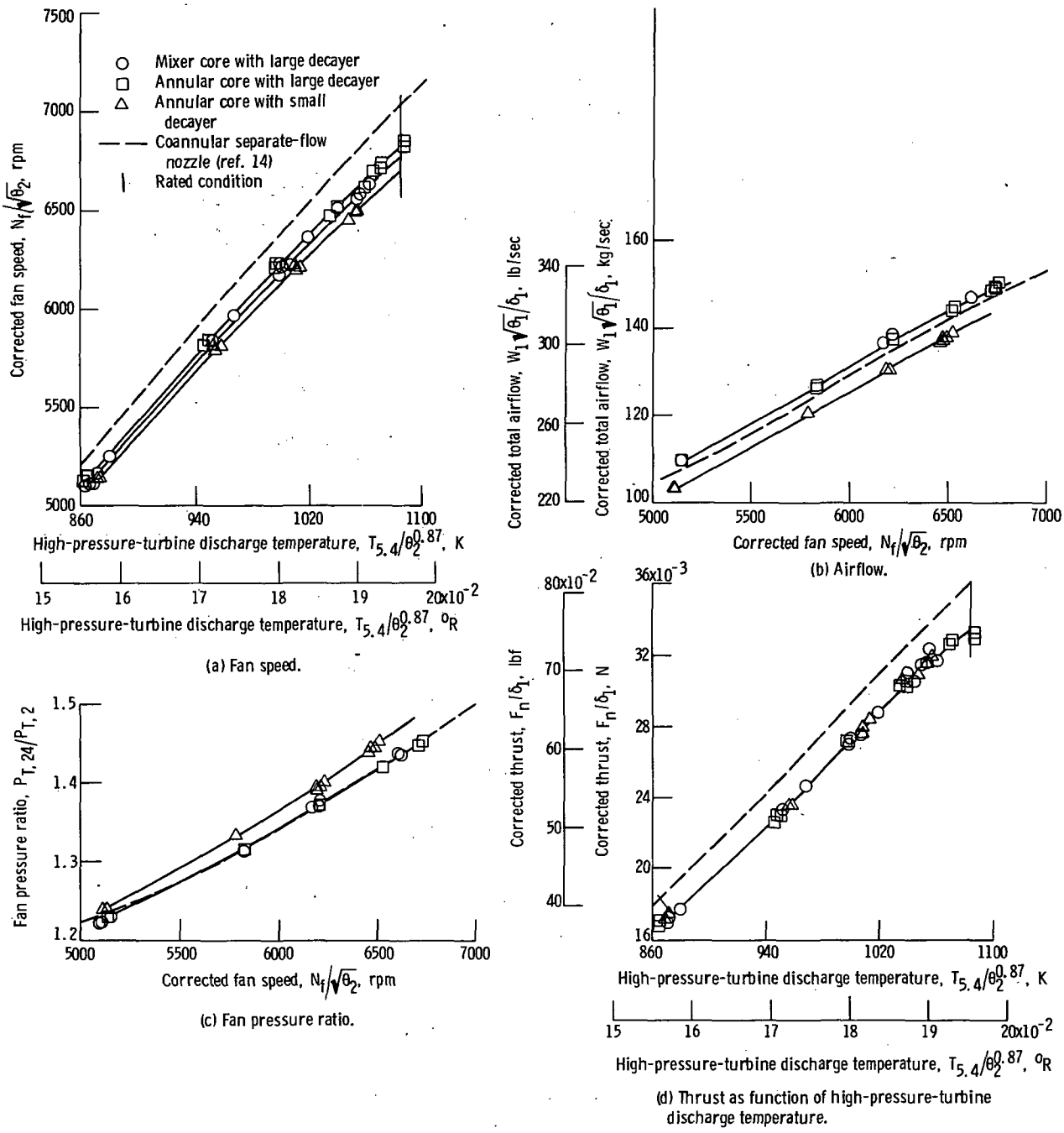

Figure 23. - Engine performance characteristics.

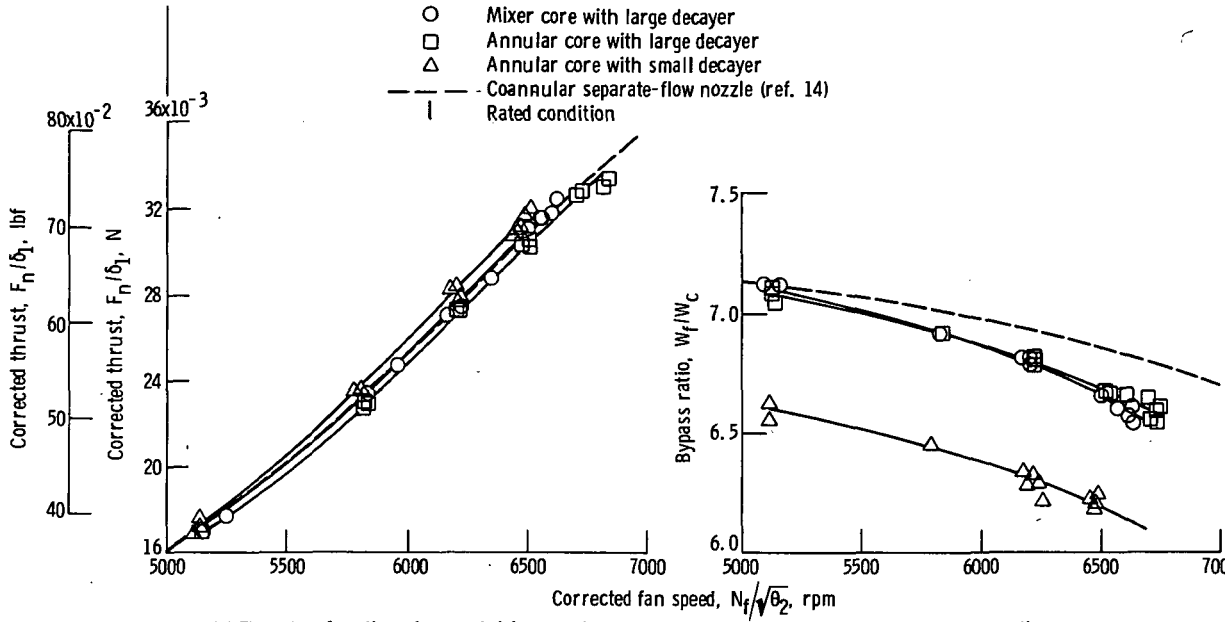

(e) Thrust as function of corrected fan speed.

(f) Bypass ratio.

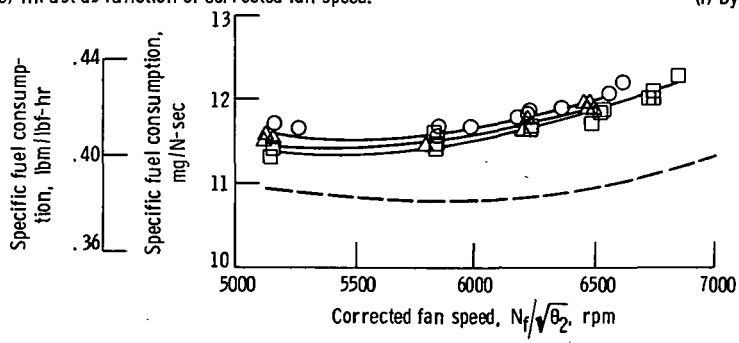

(g) Specific fuel consumption.

Figure 23. - Concluded.

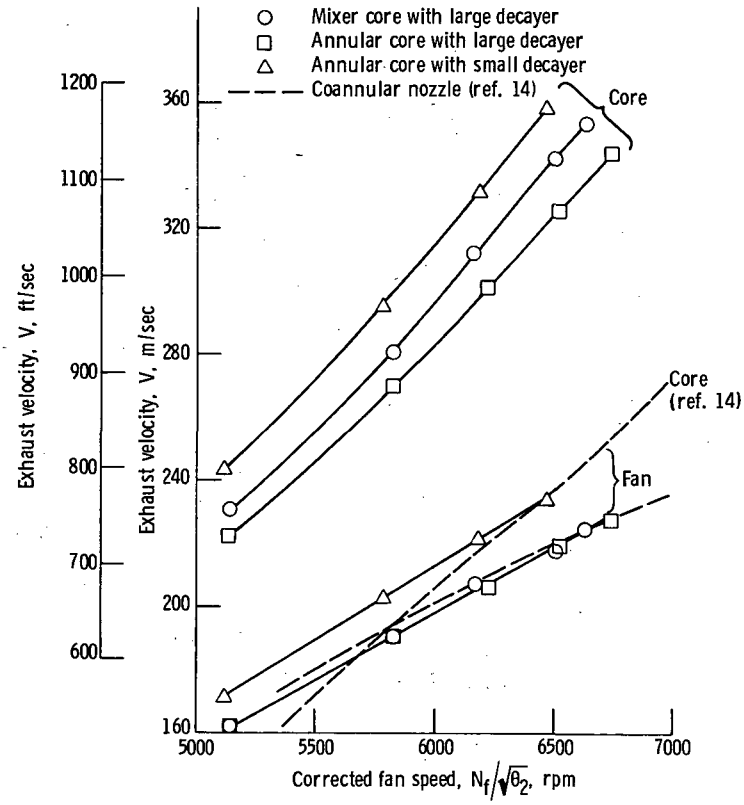

Figure 24. - Variation of fan and core exhaust velocity with fan speed.

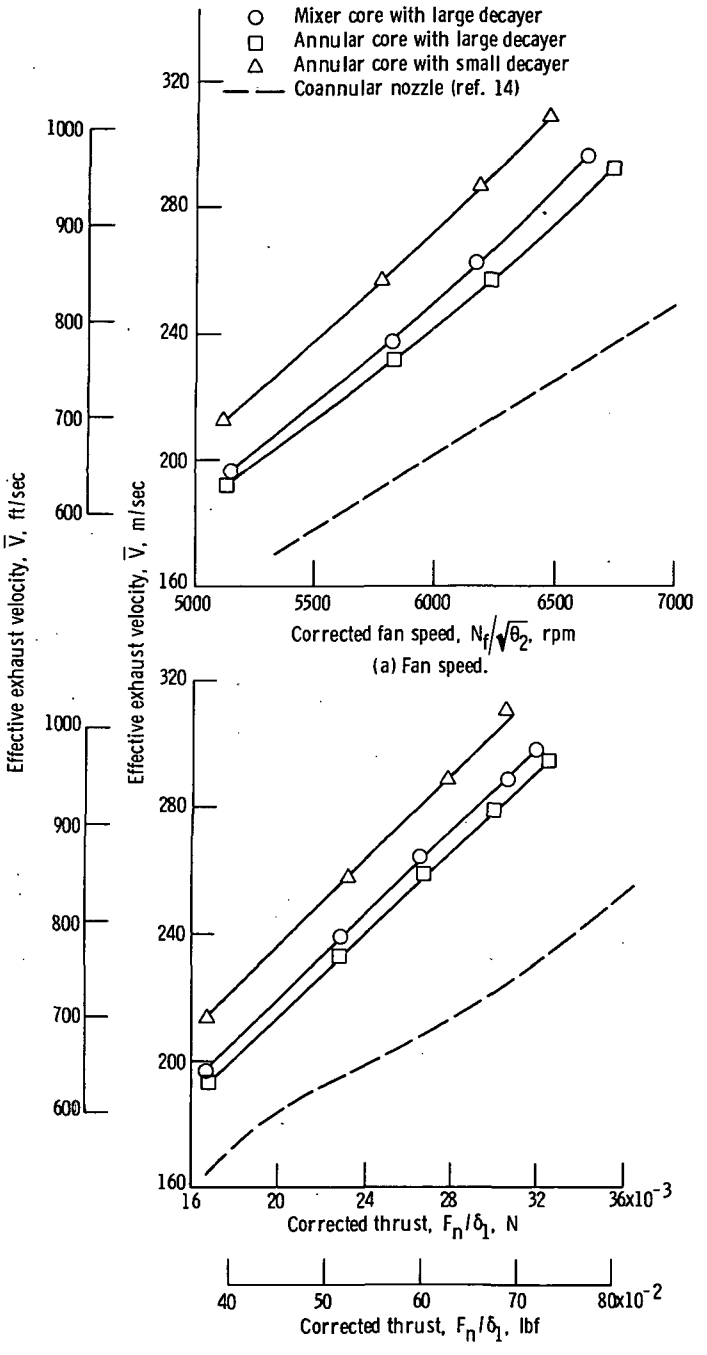

Figure 25. - Variation of effective exhaust velocity with fan speed and engine thrust.

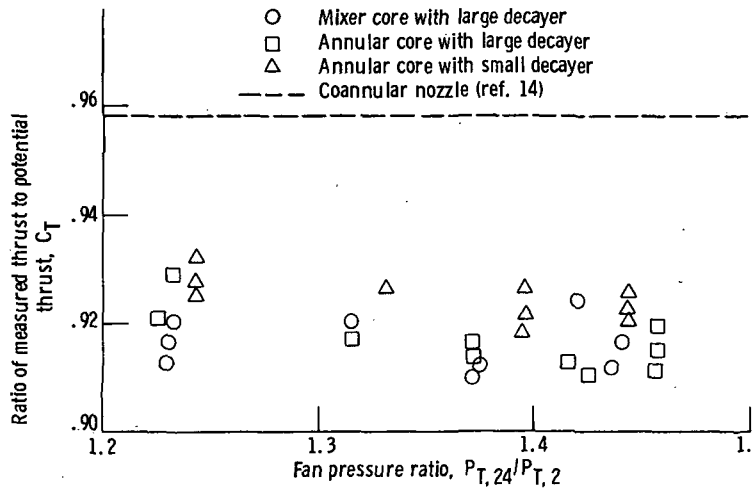

Figure 26. - Exhaust nozzle efficiency.

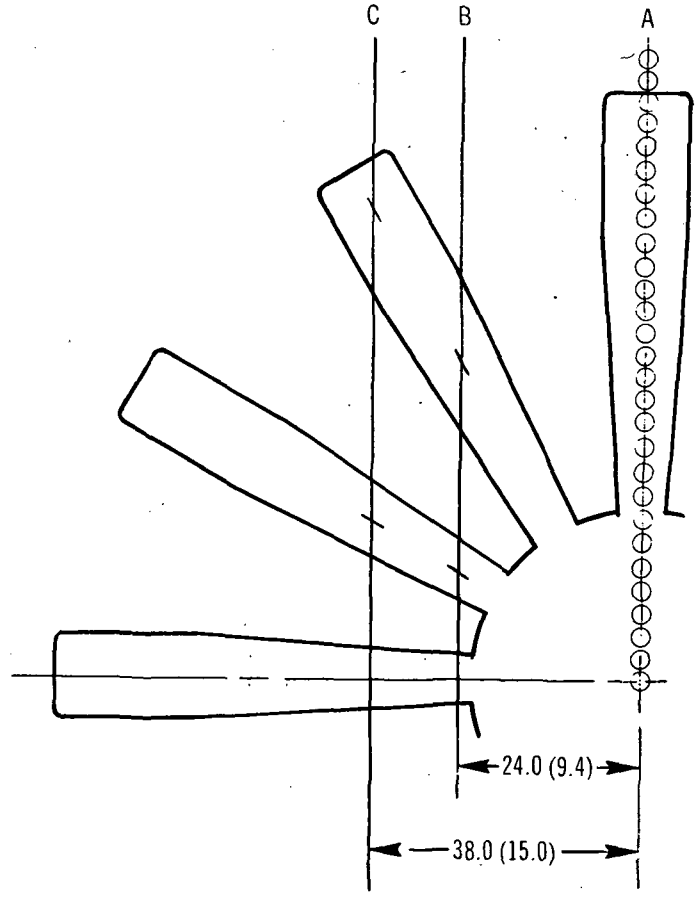

Figure 27. - Rake positions for exhaust plume velocity determination. (All dimensions are in cm (in.).)

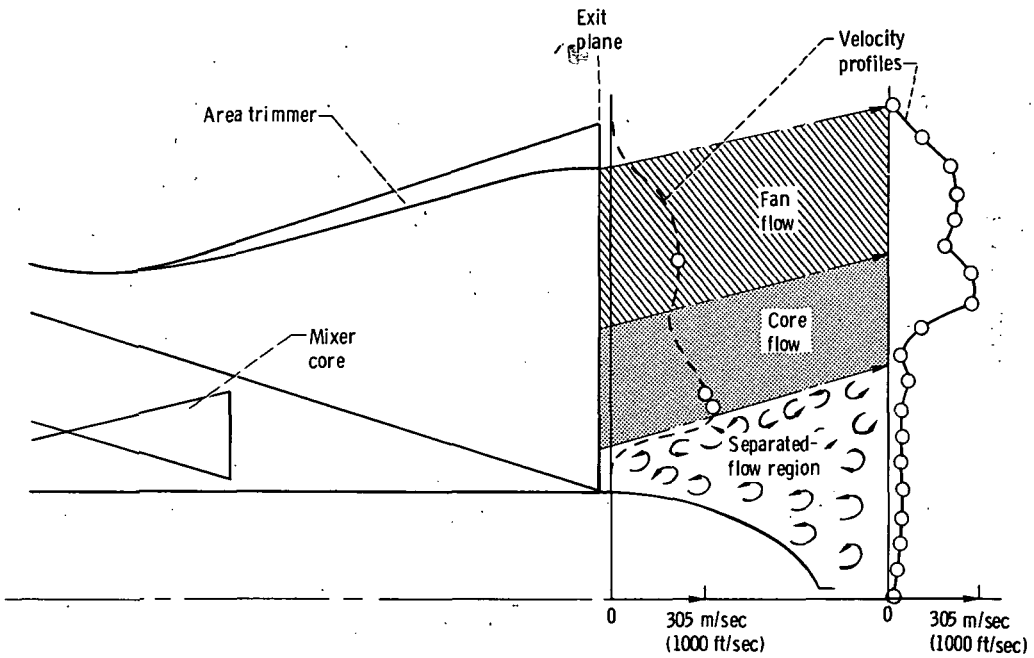

Figure 28. - Flow field at exit of decayer nozzle.

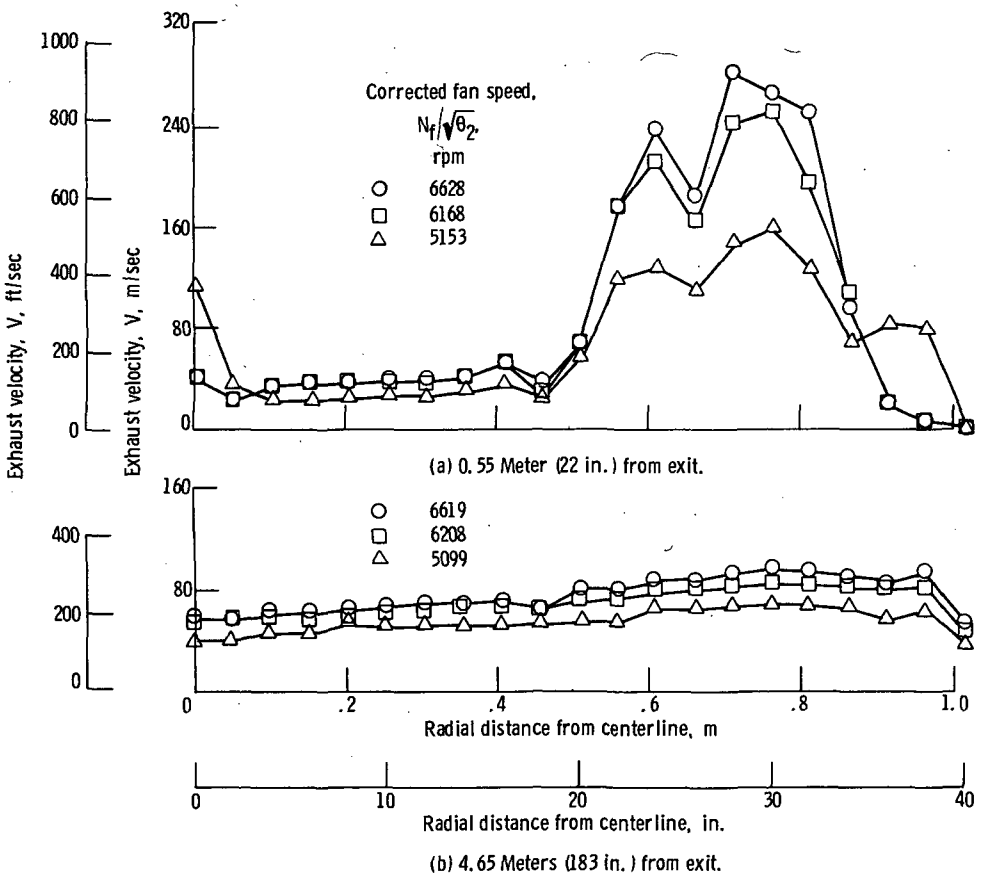

Figure 29. - Exhaust velocity profiles directly behind lobe for mixer core with large decayer. Rake position A.

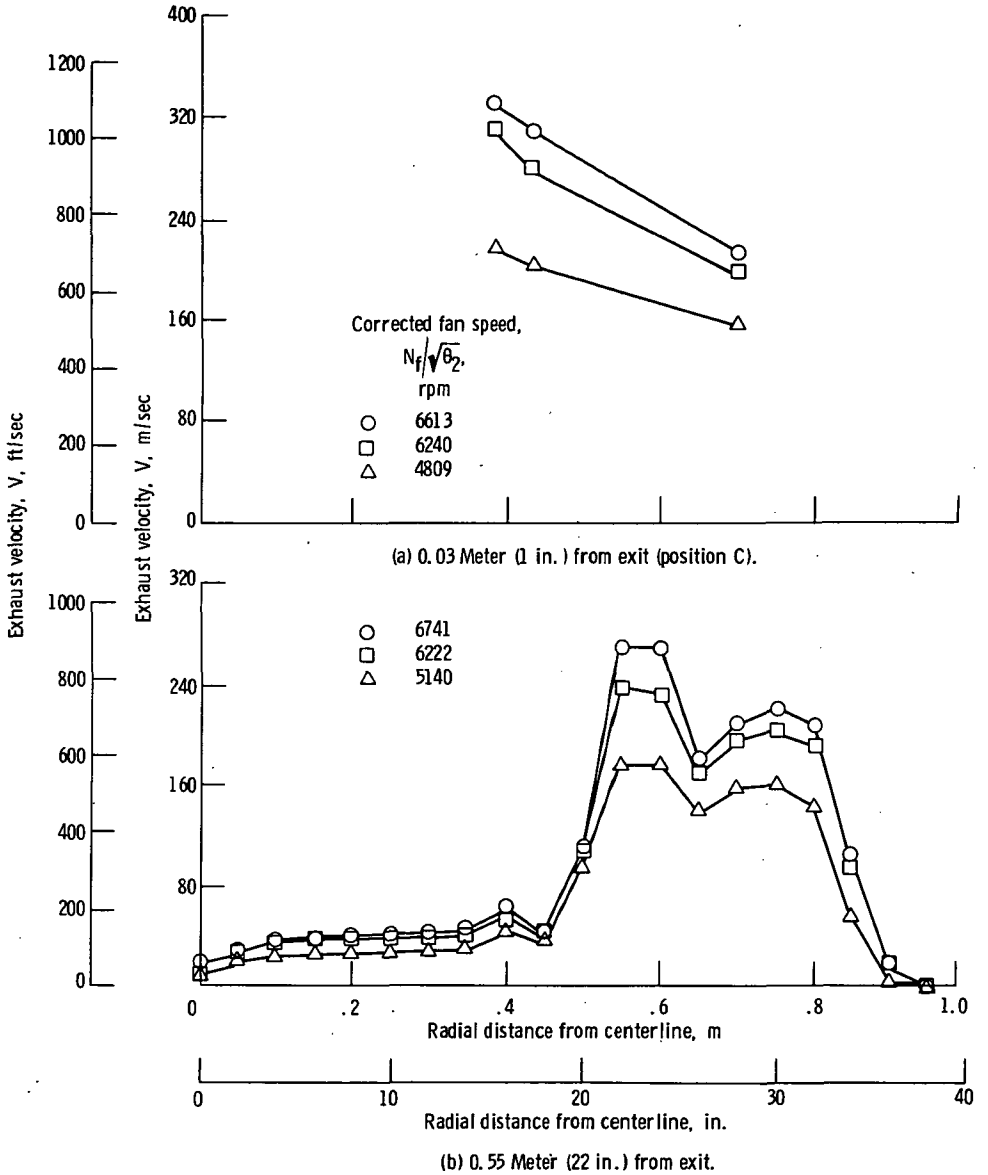

(a) 0.03 Meter (1 in.) from exit (position C).

(b) 0.55 Meter (22 in.) from exit.

Figure 30. - Exhaust velocity profiles directly behind lobe for annular core with large decayer.

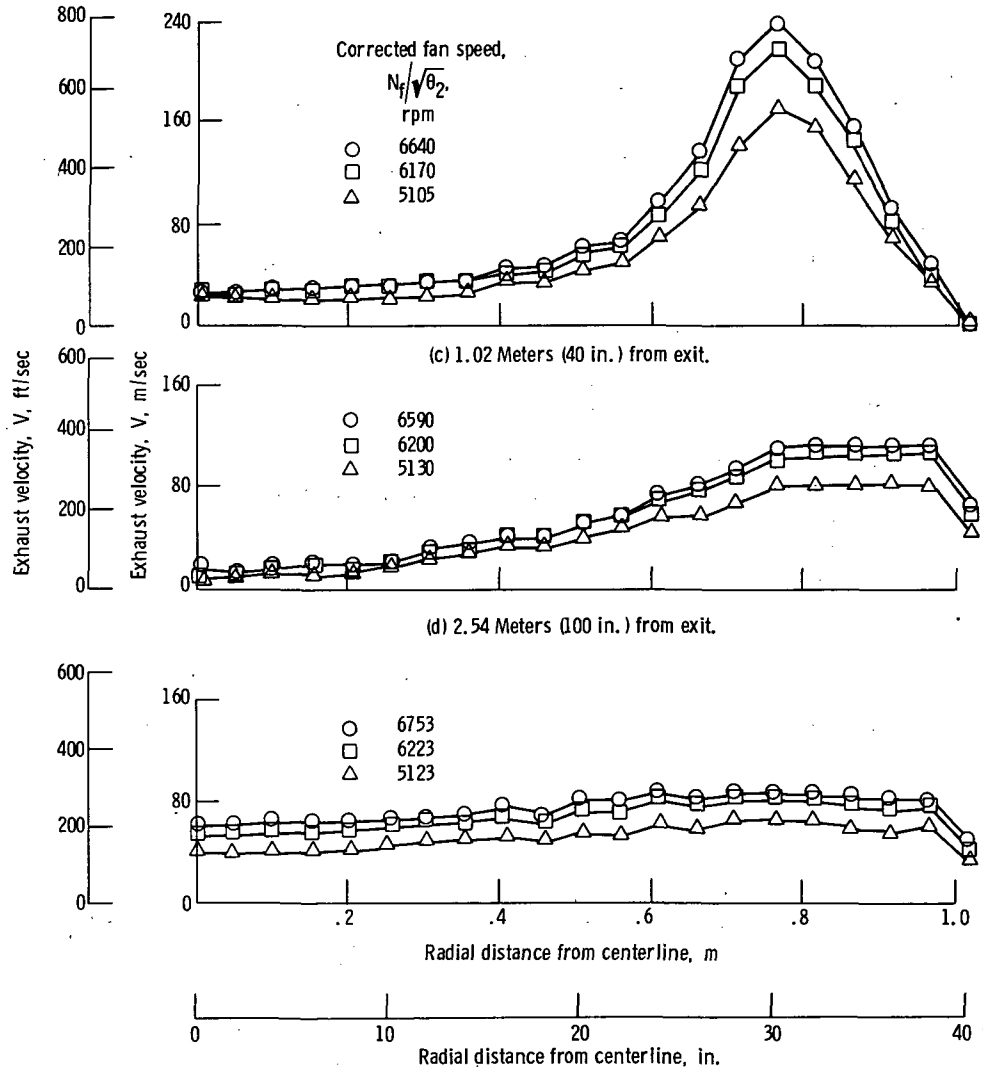

(c) 1.02 Meters (40 in.) from exit.

(d) 2.54 Meters (100 in.) from exit.

(e) 4.65 Meters (183 in.) from exit.

Figure 30. - Concluded.

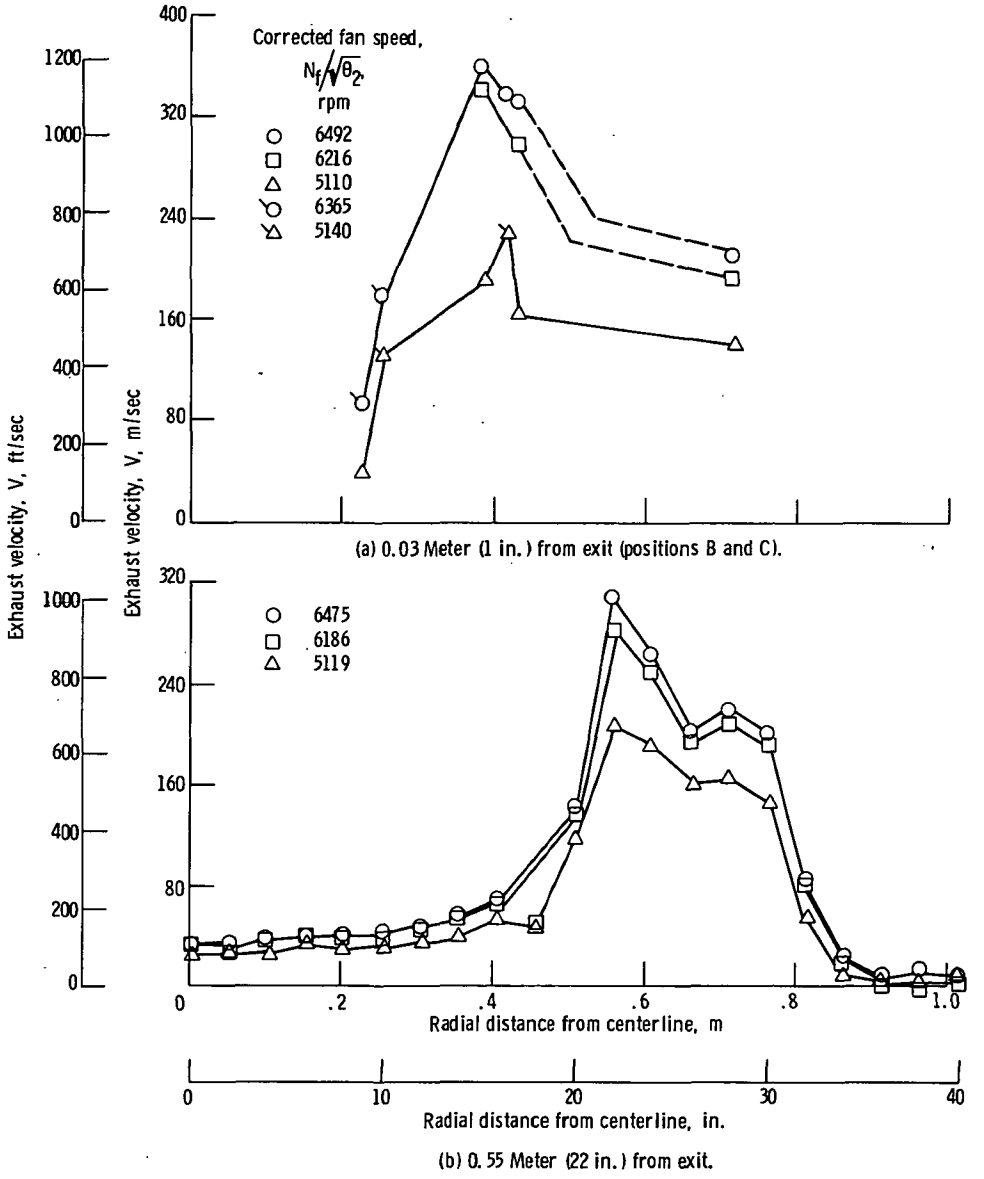

(a) 0.03 Meter (1 in.) from exit (positions B and C).

(b) 0.55 Meter (22 in.) from exit.

Figure 31. - Exhaust velocity profiles directly behind lobe for annular core with small decayer. Rake position A.

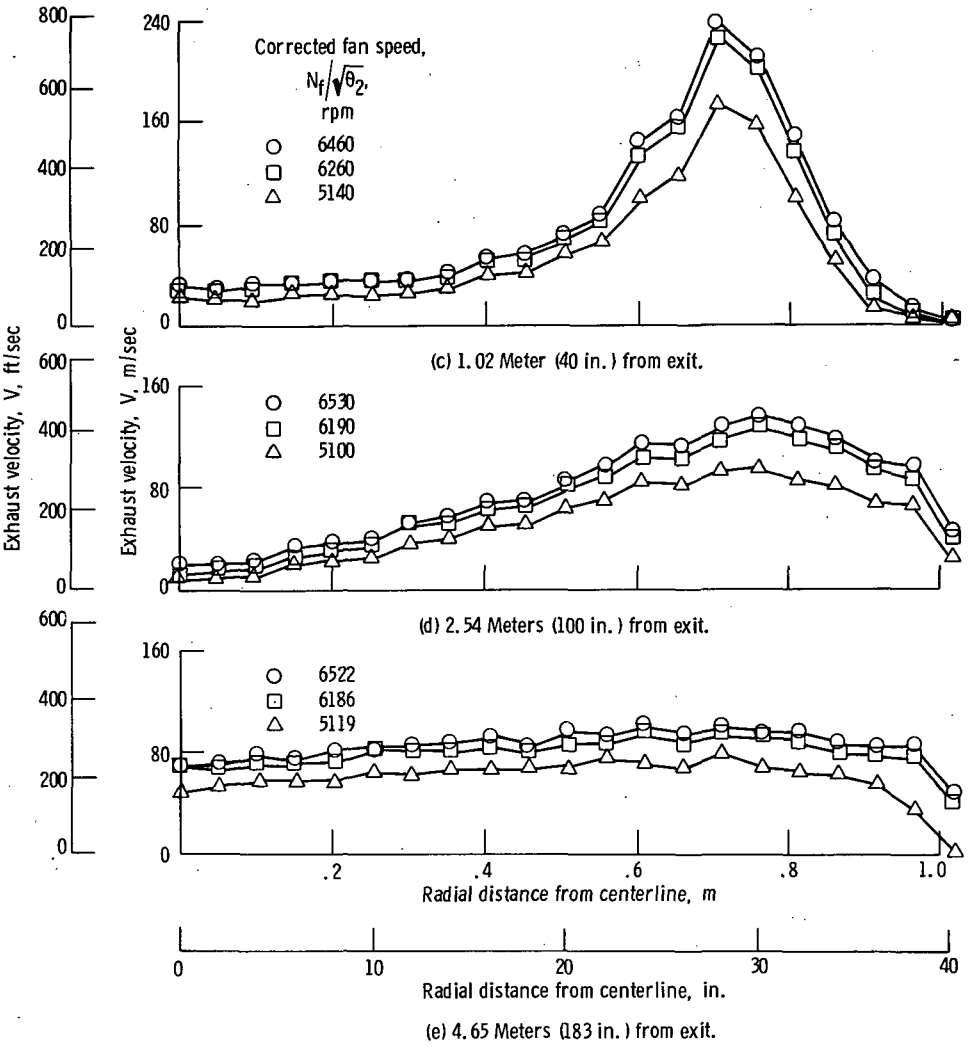

(c) 1.02 Meter (40 in.) from exit.

(d) 2.54 Meters (100 in.) from exit.

(e) 4.65 Meters (183 in.) from exit.

Figure 31. - Concluded.

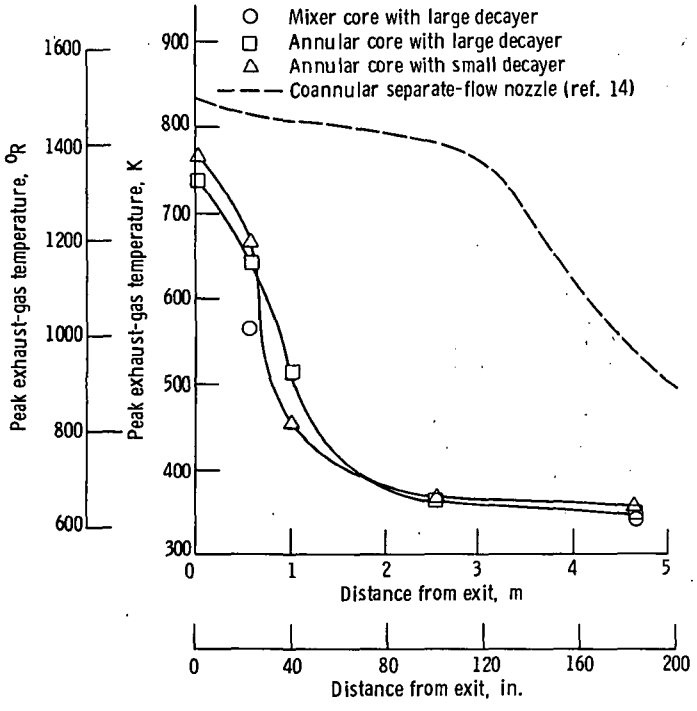

Figure 32. - Peak exhaust-gas temperature decay with distance from exit. Temperature at outlet of low-pressure turbine, T_6, 847 K (1525° R).

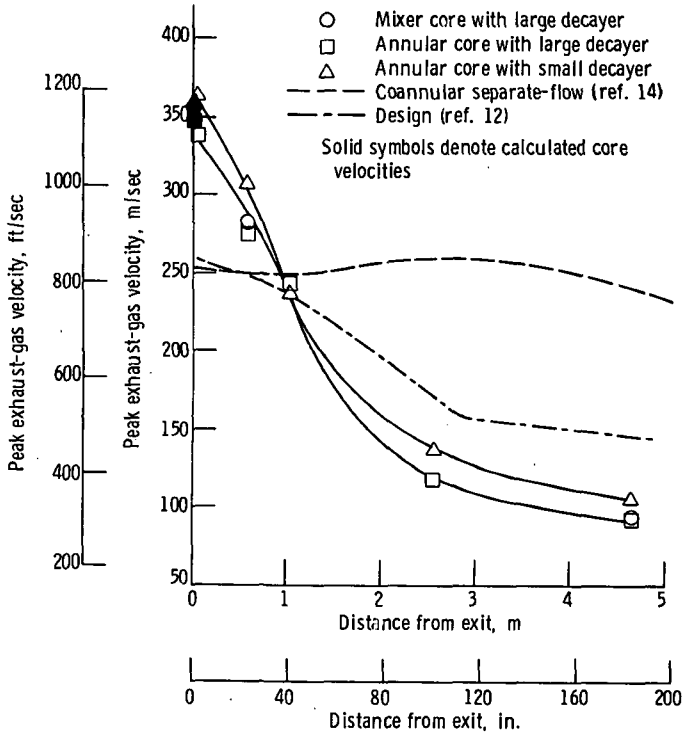

Figure 33. - Peak exhaust-gas velocity decay with distance from exit in centimeters. Temperature at outlet of low-pressure turbint, T_6, 847 K (1525° R).

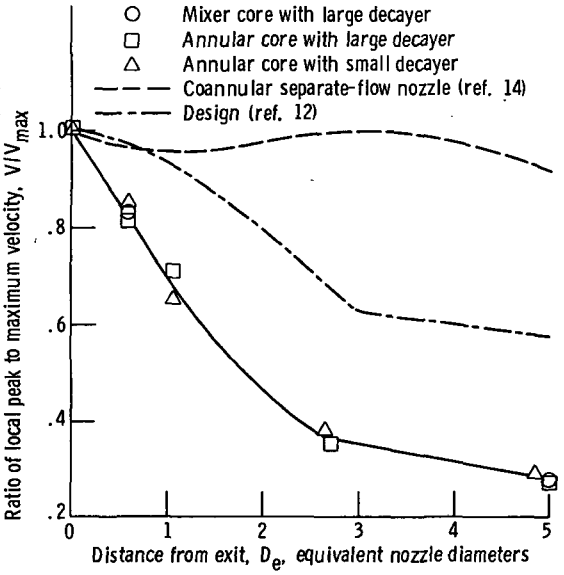

Figure 34. - Peak exhaust-gas velocity decay with distance from exit in equivalent nozzle diameters. Temperature at station 6, T_6, 847 K (1525° R).

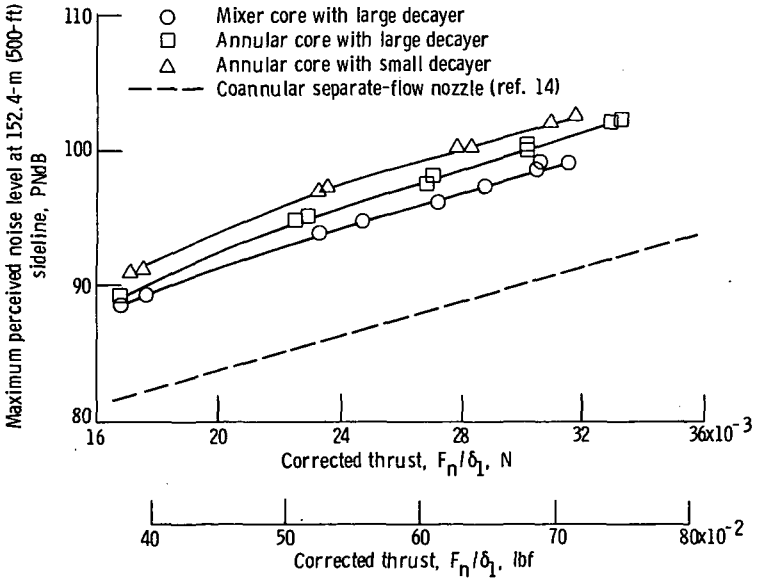

Figure 35. - Variation of sideline noise with engine thrust.

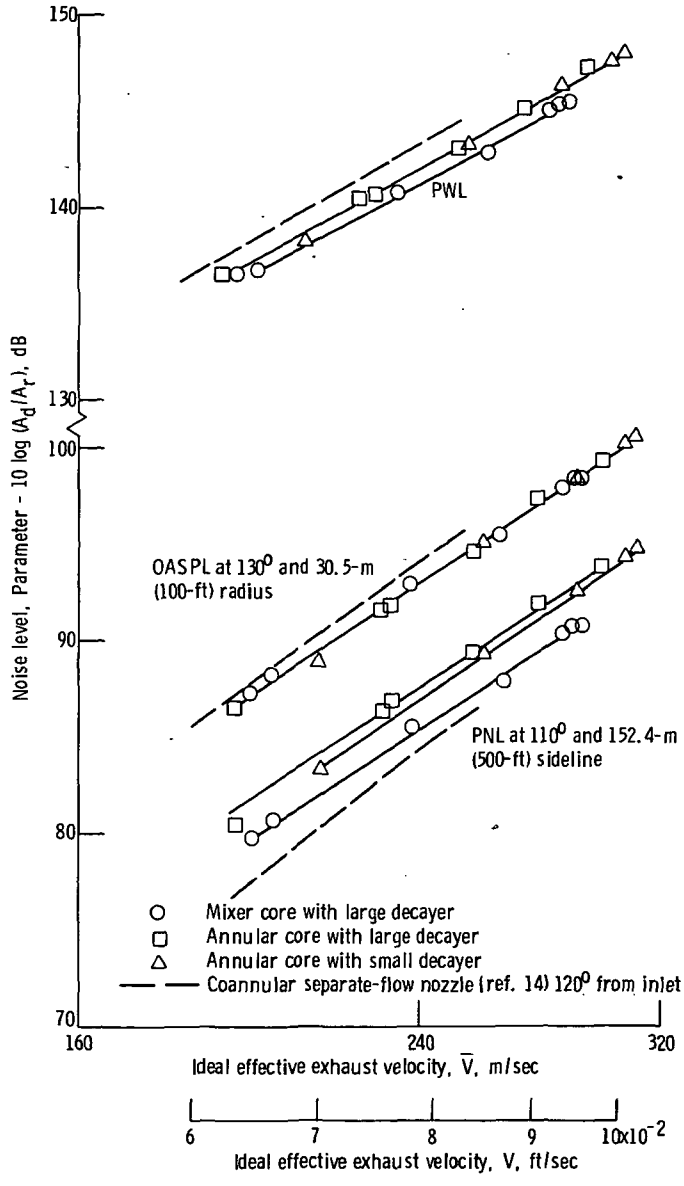

Figure 36. - Variation of acoustic characteristics with effective exhaust velocity. Reference area, A_r, 0.095 m^2 (1 ft^2).

NATIONAL AERONAUTICS AND SPACE ADMINISTRATION
WASHINGTON, D.C. 20546

OFFICIAL BUSINESS
PENALTY FOR PRIVATE USE $300

SPECIAL FOURTH-CLASS RATE BOOK

POSTAGE AND FEES PAID
NATIONAL AERONAUTICS AND SPACE ADMINISTRATION
451

U.S.MAIL

POSTMASTER : If Undeliverable (Section 158 Postal Manual) Do Not Return

"The aeronautical and space activities of the United States shall be conducted so as to contribute . . . to the expansion of human knowledge of phenomena in the atmosphere and space. The Administration shall provide for the widest practicable and appropriate dissemination of information concerning its activities and the results thereof."

—NATIONAL AERONAUTICS AND SPACE ACT OF 1958

NASA SCIENTIFIC AND TECHNICAL PUBLICATIONS

TECHNICAL REPORTS: Scientific and technical information considered important, complete, and a lasting contribution to existing knowledge.

TECHNICAL NOTES: Information less broad in scope but nevertheless of importance as a contribution to existing knowledge.

TECHNICAL MEMORANDUMS: Information receiving limited distribution because of preliminary data, security classification, or other reasons. Also includes conference proceedings with either limited or unlimited distribution.

CONTRACTOR REPORTS: Scientific and technical information generated under a NASA contract or grant and considered an important contribution to existing knowledge.

TECHNICAL TRANSLATIONS: Information published in a foreign language considered to merit NASA distribution in English.

SPECIAL PUBLICATIONS: Information derived from or of value to NASA activities. Publications include final reports of major projects, monographs, data compilations, handbooks, sourcebooks, and special bibliographies.

TECHNOLOGY UTILIZATION PUBLICATIONS: Information on technology used by NASA that may be of particular interest in commercial and other non-aerospace applications. Publications include Tech Briefs, Technology Utilization Reports and Technology Surveys.

Details on the availability of these publications may be obtained from:

SCIENTIFIC AND TECHNICAL INFORMATION OFFICE

NATIONAL AERONAUTICS AND SPACE ADMINISTRATION

Washington, D.C. 20546